Spectrochimica Acta Part A: Molecular and Biomolecular Spectroscopy xxx (xxxx) xxx

Contents lists available at ScienceDirect

Spectrochimica Acta Part A: Molecular and Biomolecular Spectroscopy

journal homepage: www.elsevier.com/locate/saa

Molecular interaction of sulfonamides and ovalbumin, an allergenic egg protein, exploring biophysical, theoretical and biological studies

Ana Carolina Fradique de Lyra, Amanda L. dos Santos Silva, Elane Cristina L. dos Santos, Ana Maria Queijeiro López, Júlio Cosme S. da Silva, Isis Martins Figueiredo, Josué Carinhanha Caldas Santos *

Institute of Chemistry and Biotechnology, Federal University of Alagoas, Campus A. C. Simões, 57072-900 Maceió, Alagoas, Brazil

ARTICLE INFO

Article history:
Received 3 August 2019
Received in revised form 27 October 2019
Accepted 1 November 2019
Available online xxxx

Keywords:
Ovalbumin
Veterinary antibiotics
Allergenicity

ABSTRACT

Biophysical, theoretical and biological *in vitro* studies were carried out to evaluate the interaction of the main allergen protein of egg white (ovalbumin, OVA) with sulphonamides (SA): sulphathiazole (S1), sulfaquinoxaline (S2), sulfadimethoxine (S3) and sulfamethazine (S4). The binding constants for the OVA-SA supramolecular complexes ranged from 1.20 to 30.66 × 10^5 M^{-1}, observing the following order of affinity: S1 > S2 > S4 > S3. The preferential forces in the stabilization of the OVA complexes with S2 and S3 were hydrogen bonds and Van der Waals forces, whereas for OVA-S1 and OVA—S4, were electrostatic interactions. Interaction process led to a change in the native structure of the protein, which may potentiate its natural allergenicity. Cations Ca (II), Mg(II) and Fe(III) favor the interaction of OVA with S1 and S2. The theoretical studies performed were consistent with the spectroscopic data. Finally, it was found that the interaction process for sulfonamides evaluated with OVA change the inhibition activity profile these antibiotics against strains of *Escherichia coli* ATCC 25922 and *Bacillus megaterium* APFSG3isox, but not the minimal inhibitory concentration values.

© 2019 Elsevier B.V. All rights reserved.

1. Introduction

Ovalbumin (OVA), the main natural allergen present in eggs, is a phosphoglyco protein with a three-dimensional arrangement consisting of nine α-helices, three β-sheets and 385 amino acid residues with approximately 45 kDa [1,2]. The ovalbumin corresponds to 54% of the total protein content of egg white in mass and, therefore, is the major protein of this food. In addition to the OVA, >40 types of proteins can be found in the egg white, among which ovotransferrin, ovomucoid, ovomucine and lysozyme may be mentioned [3].

Due to its excellent functional properties, such as emulsification, gelation and foam formation [4], ovalbumin has great industrial relevance and is widely used in the processing of various types of food. However, according to Caubet et al. [5] significant amounts of this protein can be found in vaccines made from the use of chicken eggs, such as vaccines against influenza virus, yellow fever and triple viral (measles, mumps and rubella). Influenza vaccines based on virus cultured and isolated from embryonated and then inactivated chicken eggs have been widely used for over 60 years due to cost/benefit. However, even when this process is established and with a long time of execution, it is not exempt from inducing allergic reactions in individuals hypersensitive to egg components [6,7].

Allergic reactions associated with chicken egg, a food widely distributed in the population because of its high nutritional value and low cost, are the second most common food allergy in infants and children, after allergic reactions related to milk proteins [5]. Ovalbumin is the main natural allergen in the egg, which induce an immunoglobulin E (IgE) mediated reaction, where the body recognizes the allergen as a foreign species and activates the immune system [8–10]. Macromolecule-binding interaction studies demonstrate that non-covalent interactions between ovalbumin and different ligands [11–18] may induce conformational changes in the native protein structure, which may induce or potentiate the allergic reaction.

Thus, in this work, the interaction of OVA with four sulfonamides (SA): sulphathiazole (S1), sulfaquinoxaline (S2), sulfadimetoxin (S3) and sulfametazine (S4) was studied. Sulfonamides are antibiotics mainly used in veterinary medicine due to the low cost and broad spectrum of action on Gram positive, Gram negative and protozoan bacteria [19,20]. In the Scheme 1 (supplementary material) the chemical structures of SA used in this work are presented, which differ from each other according to the substituent -R linked to the nitrogen of the sulfonic amide.

Sulfonamides (S1, S2, S3 and S4) are widely used as a therapeutic agent in poultry, especially chickens, for the control of diseases [21]. Mehtabuddin et al. [22] and Xu et al. [23] verified residual levels of these antibiotics in egg and meat samples, which were higher than those allowed by control organs. Thus, according to Silva et al. [20] the

* Corresponding author.
E-mail address: josue@iqb.ufal.br (J.C.C. Santos).

https://doi.org/10.1016/j.saa.2019.117747
1386-1425/© 2019 Elsevier B.V. All rights reserved.

indiscriminate use of veterinary drugs in food-producing animals such as eggs can generate residues in them and result in toxic effects, allergic reactions and resistance to antibiotics to consumers. In addition, the protein-antibiotic interaction process may also alter its efficiency.

Interaction studies of these antibiotics have previously been reported with bovine serum albumin (BSA) and human serum albumin (HSA) [24–27]. However, studies on the interaction of SA with food proteins are still absent, so that the purpose of this work was the interaction of ovalbumin, with four sulfonamides, using spectroscopic techniques, theoretical studies and antimicrobial activity assays to evaluate the possible conformational changes in the protein structure to understand the protein-ligand interaction process, simulating food under physiological conditions.

2. Experimental

2.1. Reagents and solutions

The commercial ovalbumin similar of the food composition (the main protein from chicken egg white, containing 62–88%), the antibiotics sulfatiazol, sulfaquinoxaline, sulfadimetoxin and sulfametazine, Tris-HCl, 8-anilino-1-naphthalenesulfonate (ANS), dimethyl sulfoxide (DMSO), KH_2PO_4 and Na_2HPO_4 were all obtained from Sigma-Aldrich (USA) with analytical purity. Stock solutions of antibiotics (10 mM) were prepared by directly dissolving the appropriate amount of the solid in DMSO. The antibiotic working solutions and the commercial OVA stock solution were prepared in 50 mM Tris-HCl buffer (pH 7.4 ± 0.1) with 100 mM NaCl for ionic strength adjustment.

To prepare the solution of OVA *in natura*, 0.150 g of the albumen from white egg of large commercial grade egg (Granja Almeida, Maceió, Alagoas, Brazil) was weighed and solubilized in 30 mL of the Tris-HCl buffer solution (pH 7.4 ± 0.1), yielding a representative solution of ovalbumin. The concentration of commercial and *in natura* OVA was determined using Beer's law (280 nm) and molar extinction coefficient (ε_{280}) of 30,957 M^{-1} cm^{-1}, after dilution of 1:5 of the stock solution of the protein [2]. Ultrapure water (18.2 MΩ cm^{-1}) was used in the experiments for the preparation of solutions and buffer (Gehaka, model Mater System MS2000, Brazil).

To evaluate the biological activity, the stock solutions of the antibiotics (SA) were prepared by dissolving directly each of them in DMSO (2.5 mg mL^{-1} for S1, S2 and S4, and 1.25 mg mL^{-1} for S3). The combined solutions of each antibiotic with OVA were prepared by mixing the stock solutions of antibiotics (1:1 v/v) in OVA solution in 50 mM Tris-HCl buffer (pH 7.4 ± 0.1) containing 100 mM of NaCl (in sterile distilled water). For pH measurements, a pH meter (Gehaka, model PG 1800, Brazil) coupled to a combined glass electrode was used (±0.01 of uncertainty). Standards and reagents were weighed on an analytical balance (Mettler Toledo, model AG245, USA) with accurate to 0.01 mg.

2.2. Molecular absorption spectroscopy (UV–vis)

OVA absorption spectra (3 μM) of different SA (6 μM) and complexes (OVA + SA), using UV–vis, were obtained using a double-beam Micronal spectrophotometer (model AJX-6100PC, Brazil) equipped with quartz 1.0 cm (optical path).

2.3. Molecular fluorescence studies

In molecular fluorescence studies, steady-state fluorescence spectra were obtained by a Shimadzu spectrofluorimeter (model RF-5301PC, Japan) equipped with a 150 W xenon lamp. All spectrofluorimetric measurements were performed using a cuvette of 1.0 cm quartz (optical path) with and excitation and emission slit set at 3 and 5 nm, respectively. The intrinsic OVA (2 μM) fluorescence emission spectra in the absence and presence of the ligands (S1, S2, S3 and S4) were obtained by spectrofluorometric titration with increasing amounts of SA (0–200 μM) at pH 7.4, using $\lambda_{ex} = 280$ nm. Similarly, evaluation was performed at three temperatures (23, 30 and 37 °C) to obtain the thermodynamic parameters of the interaction process. When necessary, the protein fluorescence signal was corrected.

The three-dimensional fluorescence (3D) study was performed to evaluate possible conformational changes in the secondary structure of the protein [28]. In this study, the emission spectra of OVA intrinsic fluorescence (2 μM) in the absence and presence of different SA (40 μM) were obtained using a range of excitation length of 220–350 nm and emission of 250–450 nm. Synchronous fluorescence was performed to monitor separately the fluorophores, Tyr and Trp, present in OVA and possible changes in the polarity of their microenvironments [29]. For this, the spectra were obtained by means of the simultaneous variation of emission and excitation monochromators. The value of the $\Delta\lambda$ ($\Delta\lambda = \lambda_{em} - \lambda_{ex}$) between the emission and excitation wavelengths was kept fixed. It was applied $\Delta\lambda = 15$ nm and $\Delta\lambda = 60$ nm to monitor the spectroscopic behavior of the Tyr and Trp residues, respectively.

To calculate the critical distance between the donor (OVA fluorophores) and energy acceptor (ligands) during the interaction process of ovalbumin (2 μM) with the different SA (10 μM) the assay was performed based on Resonance Energy Transfer concept [30]. The competition studies were performed with ANS and metal ions. The competition assay with the ANS probe was performed to evaluate hydrophobic OVA sites in the presence of SA. For this purpose, titration of the OVA system (2 μM) and ANS (4 μM) was performed in the presence of different concentrations of the SA (0–200 μM) with $\lambda_{ex} = 334$ nm (OVA-ANS). Additionally, a competition study with Ca(II), Mg(II), Zn(II) and Cu(II) (derived from the respective acetates) and Fe(III) ions (from the respective chloride) all species at 2 μM was accomplished.

2.4. Molecular docking simulations

The initial coordinates of ovalbumin protein used for molecular docking simulations were obtained from a crystal structure with 1.95 Å of resolution deposited in the Protein Data Bank server with PDB code 1OVA. Atomic coordinates for sulfonamides S1, S2, S3 and S4 were generated from geometry optimization calculations performed using density functional theory with B3LYP [31,32] exchange-correlation functional in conjunction with 6–31 + G(d,p) [33] basis set functions. All geometry optimizations and frequency calculations were carried out using the C.01 version of Gaussian 09 program [34]. Molecular docking simulations were performed using Autodock4 [35,36] and AutoDockTools [37] programs, were the atomic partial charges of protein and ligands were calculated by using Gasteiger method [38,39]. In this present work, we applied a conventional docking simulation protocol used in previous works [40–42]. Thus, all protein-sulfonamides systems were simulated *via* grid maps with 129 × 129 × 129 points and grid-point spacing of 0.25 Å. The simulations were carried out using the Lamarckian genetic algorithm with an initial population of 150 random individuals and a maximum number of 2.5×10^6 energy evaluations. In each case were generated a maximum number of 2.7×10^4 generations with rates of gene mutation and crossover of 0.02 and 0.8, respectively. A maximum of 300 iterations per local search was allowed. These local searches were performed considering a probability on an individual of 0.06. The coordinates of the lowest energy conformations were clustered based on a root-mean-squared-deviation of 2.0 Å.

2.5. Biological antimicrobial activity

In order to evaluate the antimicrobial potential *in vitro* of the different SA linked to the ovalbumin protein, antibiograms were performed by the Kirby-Bauer disk-diffusion method [43,44], using five bacterial strains selected from the collection of the "Laboratory of Biochemistry of Parasitism and Environmental Microbiology - Institute of Chemistry and Biotechnology (LBPMA/IQB)", at the Federal University of Alagoas

(UFAL, Brazil), namely: *Escherichia coli* ATCC 25922 (standard strain), *Pseudomonas aeruginosa* ATCC 27853 (standard strain), *Corynebacterium glutamicum* (LBPMA), *Klebsiella oxytoca* BMA-13 and *Bacillus megaterium* APFSG3isox (the latter two with deposition of their 16S r-RNA sequences in GenBank NCBI, accession numbers respectively KU555927 and KX129778).

2.5.1. Preparation and inoculation of the nutrient agar (NA) maintenance medium

For the maintenance of active cells of the selected bacterial strains, a colony (reared) of each original pure culture (at 6 ± 2 °C, in the dark) was seeded (by striations) in sterilized (120 °C, 20 min) nutrient agar medium (NA, composition in distilled water in g L^{-1}: peptone, 5; meat extract, 3; sodium chloride, 1; agar, 20) and contained in Petri dishes. Cultures were incubated for 24 h (at 32 ± 1 °C, in the dark).

2.5.2. Antimicrobial assay in Mueller Hinton agar (MHA) medium

Bacterial suspensions of strains cultured for 24 h in NA were previously obtained to inoculate the MHA medium through the *pour plate* technique. To this end, a 10 mL volume of sterilized distilled water was deposited on the surface of each culture and with the aid of a Drigalsky loop, the suspension of cells was homogenized. After that, it was harvested in the sterilized tube using an equally sterilized Pasteur pipette. The concentration of cells from each suspension was determined using the Mc Farland scale. Then, the suspensions were diluted to 20 mL and transferred to 200 mL of the previously sterilized and still liquefied MHA medium (HiMedia®; 38 g L^{-1}distilled water), yielding the concentration of 2.77×10^7 cells mL^{-1}. The inoculated medium was poured into Petri dishes (θ ≅ 9 or 18 cm; thickness of medium ≅ 4–5 mm).

After that, a filter paper disc containing the standard ofloxacin (5 μg) antibiotic, as well as new sterilized preparatory filter paper disks were placed on the surface of the MHA medium, in equidistant positions thereto and from each other and from the edges. Aliquots of OVA diluents (DMSO and Tris-HCl buffer) and individual and/or OVA-complexed antibiotics were then collected with sterile pipette and deposited on the paper discs. In a preliminary test in duplicates ($n = 2$) using the smaller plaques (for *E. coli*, *B. megaterium* and *P. aeruginosa*), seven disks were added - one for the ofloxacin standard and the other for pure DMSO, the buffer and the four SA; or eight disks - one for the standard ofloxacin and the other for pure DMSO, buffer, OVA, the four SA plus the four OVA-SA systems. In the case of *C. glutamicum* and *K. oxytoca* inoculated in the larger plates, 12 discs were distributed referring to the standard ofloxacin, pure DMSO, buffer, OVA, different SA and different OVA-SA interaction systems. After deposition of 40 μL of the solutions on the filter paper discs (containing 100 μg of S1, S2, S4 and 50 μg for the respective systems related to the interaction process OVA—S1, OVA-S2 and OVA—S4, and 50 μg for S3 and 25 μg of the OVA-S3 system), the plates were incubated for 24 h (at 30 ± 1 °C, in the dark). Subsequently, the inhibition halos were measured with the aid of a pachymeter, and their means with the respective standard deviations were determined. According to the results obtained in the preliminary test, the other tests were carried out to establish the minimum inhibitory concentration (MIC) for the bacteria evaluated, and the systems were prepared with smaller plates containing only six disks, that is, in addition to the controls, a single SA and their interaction with OVA by concentration replication. All assays were performed in duplicate.

3. Results and discussion

3.1. Binding and thermodynamic parameters associated with the interaction process

To evaluate the interaction between the OVA and the different sulfonamides (S1, S2, S3 and S4), a spectrofluorometric titration was carried out in which the intrinsic OVA fluorescence was monitored from the nine tyrosine residues and three tryptophan residues [45]. The fluorescence intensity of free OVA (2 μM) was monitored at 336 nm after excitation at 280 nm, in the absence and presence of different concentrations of sulfonamides (0–200 μM), as can be seen in Fig. 1a, for the OVA-S1 system. A 100-fold excess of sulfonamides in relation to ovalbumin concentration was used to ensure saturation of protein binding sites. Similar results were obtained for S2, S3 and S4 (Fig. S1a–c, supplementary material). As the concentration of S1 increased, the quenching process occurred, that is, suppression of the fluorescence signal induced by the interaction of the protein with the quencher, and it was thus possible to infer that OVA interacts with S1 forming a complex non-fluorescent supramolecular OVA-S1 [46].

An evaluation at different temperatures (23, 30 and 37 °C) was performed to determine the interaction parameters (binding and thermodynamics) associated to this process. The data associated with the fluorescence quenching process were analyzed by the Stern-Volmer equation [11]:

$$\frac{F_0}{F} = 1 + K_{SV}[Q] = 1 + K_q\tau_0[Q] \quad (1)$$

in which F_0 and F correspond to the fluorescence intensities in the absence and presence of quencher, respectively, K_{sv} is the Stern-Volmer constant, [Q] is the concentration of quencher (sulfonamides), K_q is the biomolecular quenching rate constant and τ_0 is the average life time (10^{-8} s) [47,48]. Eq. 1 was applied to determine K_{sv} and K_q by linear regression from the graph of F_0/F *vs* [Q] (Fig. 1b). The data obtained at the three temperatures evaluated are shown in Table 1.

By the variation of the K_{SV} values as a function of the temperature it is possible to infer about the preferential quenching mechanism. According to Mei et al. [49], the quenching process can occur by, static or dynamic quenching mechanism, which can be differentiated by temperature dependence. At higher temperatures there is a faster diffusion of the molecules and, consequently, larger amounts of collisions between the ligand and fluorophore, characterizing the dynamic quenching process (K_{SV} increase). On the other hand, static quenching is characterized for destabilization of a non-fluorescent complex in the ground state at higher temperatures destabilized [50]. According to Table 1, the values of K_{SV} decreased with increasing temperature, thus, the preferably mechanism of interaction OVA-SA is by static quenching. Moreover, since the values obtained for K_q (Table 1) are higher than 2.0×10^{10} M^{-1} s^{-1} (0.86 to 4.19×10^{12} M^{-1} s^{-1}), it is confirmed that the static quenching is occurring [51].

In addition to the quenching constant (K_{sv} and K_q), it was also possible to determine two other binding parameters associated with protein-ligand interaction. To do so, the following equation was used:

$$\log\left(\frac{F_0 - F}{F}\right) = K_b + n\ \log[Q] \quad (2)$$

in which K_b is the binding constant related to the interaction force between OVA and sulfonamides, and *n* is the number of binding sites of the complex formed [52]. Eq. 2 was applied to determine K_b and *n* by linear regression from the log[(F_0 - F)/F] *vs* log[sulfonamide] (Fig. 1c). The data obtained in the three temperatures evaluated are presented in Table 1. From the values of K_b, it is observed that the magnitude of the interaction followed the following order: S1 > S2 > S4 > S3. Sulphathiazole (S1) was therefore the sulphonamide that interacted more effectively with OVA, whereas sulphadimethoxine (S3) showed the lowest interaction. Probably the degree of affinity of SA with OVA is related to the radical -R (Scheme S1), since less voluminous radicals (such as thiazole in S1) allow a more effective interaction, whereas more voluminous radicals should make it difficult to formation of the supramolecular complex, resulting in a lower value for K_b, as is the case of S3. The same order of affinity was obtained in the study using

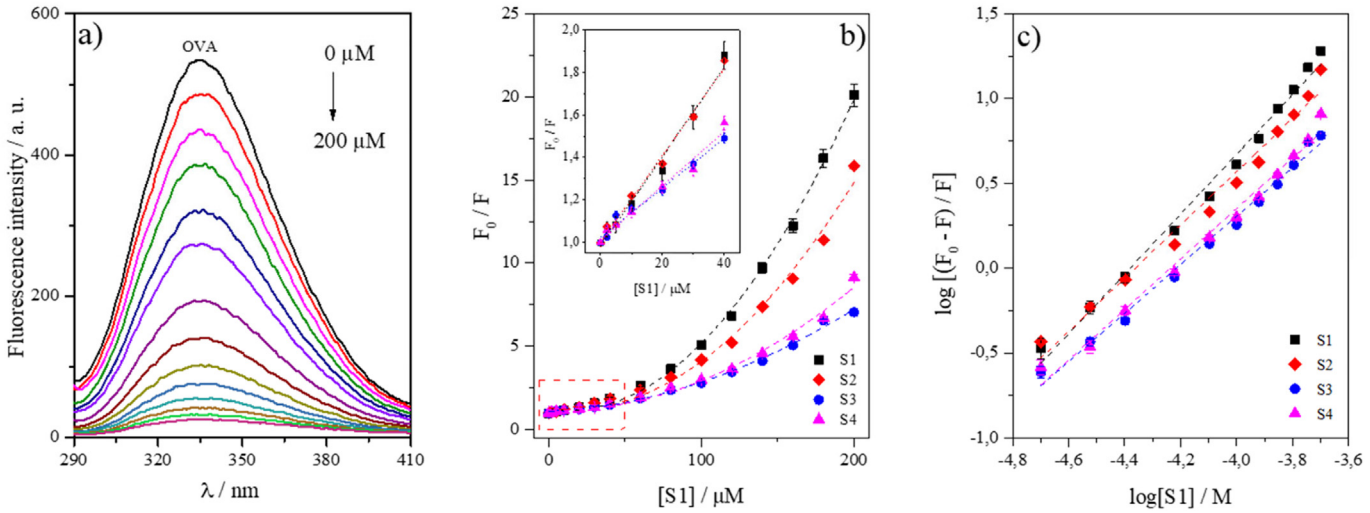


Fig. 1. a) Spectral profile of OVA in spectrofluorometric titration (2 μM) with sulfatiazol (S1), b) Linearization of the Stern-Volmer equation (internal graph - expansion of the concentration range with linear tendency in the rectangle), c) Double logarithmic curve for calculation of the binding constant (K_b) and number of binding sites (n). Conditions: 50 mM Tris-HCl buffer and 100 mM NaCl at pH 7.4 and 30 °C.

OVA *in natura* (egg white), in which for all SA the values of K_b were higher in the processes of interaction with OVA *in natura,* considering the comparison to commercial protein (Fig. S2). Possibly this is related to egg white being a more complex matrix, with several components, such as other macromolecules (proteins, lipids and carbohydrates), which may favor interaction [51].

Furthermore, it was observed that the K_b values obtained at 30 °C ranged from 3.98 to 27.7 × 10^5 M^{-1} for the interaction of different SA evaluated with OVA. Unfortunately, protein-ligand interaction experiments are not standardized in the literature regarding experimental conditions, thus limiting comparisons. However, the K_b values obtained to OVA-SAs were higher when compared to other sulfonamide with different proteins (Table S1, supplementary material). In addition, the values of the binding constants of OVA with other ligands are shown in Table S2 and it concludes that the protein has a higher affinity for the SA, even comparing different experimental conditions. The values obtained for n are close to one unit, thus, the stoichiometry of the complex between protein and SA is 1:1, probably indicating only a preferential binding-site of OVA with the ligands.

Based on K_b values obtained at different temperatures, it was possible to calculate the thermodynamic parameters and, in this way, to establish the main forces involved in the interaction between the OVA and the SA, besides verifying the tendency to spontaneity. By means of the Van't Hoff Equation it was possible to determine the values related to the enthalpy (ΔH) and entropy (ΔS) variation:

$$\ln K_b = -\frac{\Delta H}{R}\left[\frac{1}{T}\right] + \frac{\Delta S}{R} \quad (3)$$

in which R is the universal gas constant and T is the temperature in Kelvin (K) [53]. Eq. (3) was applied to determine ΔH and ΔS by linear regression of the graph $\ln K_b$ *vs* 1/T (Fig. S3). The values of ΔG were calculated by the following equation:

$$\Delta G = \Delta H - T\Delta S \quad (4)$$

The data obtained for the thermodynamic parameters are presented in Table 1. The negative values of ΔG indicate that the interaction process is spontaneous [54]. According to Hu et al. [55], the forces involved in the interaction of biomolecules with drugs may be electrostatic interactions, hydrogen bonds, Van der Waals forces, and hydrophobic interactions. The electrostatic interactions are responsible for stabilizing the complexes formed between S1 and S4 with OVA, since ΔH < 0 and ΔS > 0, whereas for S2 and S3 the interactions with the protein were by Van der Waals forces and hydrogen bonds, since ΔH < 0 and ΔS < 0 [56].

The nature of the attraction forces contributes K_b values for the interaction between OVA and SA. Since the electrostatic interactions are stronger, they can result in a greater affinity between the protein and

t1.1 **Table 1**
t1.2 Binding and thermodynamic parameters for the interaction between OVA and SA at different temperatures. Conditions: OVA (2 μM), SA (0–200 μM), 50 mM Tris-HCl buffer and 100 mM
t1.3 NaCl at pH 7.4.

t1.4	SA	T (°C)	Binding parameters						Thermodynamic parameters		
t1.5 t1.6			K_{SV} ($\times 10^4$ M^{-1})	r	K_q ($\times 10^{12}$ M^{-1} s^{-1})	K_b ($\times 10^5$ M^{-1})	r	*n*	ΔH (kJ mol^{-1})	ΔS (J mol^{-1} K^{-1})	ΔG (kJ mol^{-1})
t1.7	S1	23	4.19 ± 0.03	0.9871	4.19	30.6 ± 2.33	0.9935	1.42			−36.78
t1.8		30	4.08 ± 0.03	0.9808	4.08	27.7 ± 2.71	0.9784	1.43	−14.36	+75.76	−37.31
t1.9		37	3.75 ± 0.02	0.9958	3.75	23.5 ± 2.00	0.9905	1.38			−37.84
t1.10	S2	23	1.31 ± 0.04	0.9972	1.31	5.95 ± 1.78	0.9912	1.37			−32.92
t1.11		30	1.24 ± 0.04	0.9970	1.24	5.17 ± 1.90	0.9936	1.32	−48.80	−53.66	−32.54
t1.12		37	1.19 ± 0.01	0.9773	1.19	3.73 ± 1.49	0.9870	1.27			−32.17
t1.13	S3	23	1.06 ± 0.07	0.9891	1.06	4.35 ± 1.66	0.9803	1.37			−32.41
t1.14		30	0.99 ± 0.05	0.9902	0.99	3.98 ± 1.99	0.9928	1.36	−69.70	−125.99	−31.53
t1.15		37	0.86 ± 0.07	0.9809	0.86	1.20 ± 0.24	0.9937	1.22			−30.64
t1.16	S4	23	1.93 ± 0.08	0.9773	1.93	4.60 ± 1.58	0.9697	1.32			−32.09
t1.17		30	1.67 ± 0.08	0.9870	1.67	4.14 ± 1.29	0.9876	1.31	−11.57	+69.34	−32.58
t1.18		37	1.47 ± 0.01	0.9955	1.47	3.72 ± 1.82	0.9908	1.25			−33.06

the ligand and, therefore, it is justified because S1 is the sulfonamide with greater constant. While Van der Waals forces and hydrogen bonds are comparatively weaker compared to electrostatic forces, it could be the reason for a lower affinity between S3 and OVA. However, it is known that the formation of the supramolecular complex can be the result of a sum of attractive forces causing values of constants smaller or larger than predicted. This profile applies to S2 and S4, where S2 has a constant relatively greater than S4, even the latter having electrostatic interactions as preferred. Finally, one should also consider possible differences in the preferred interaction regions of each ligand relative to the protein.

The main forces related to the interactions between sulfonamides and OVA can also be explained based on the distribution of species as a function of pH, since the molecules evaluated are derived from weak acids. The profile of the species distribution graph (Fig. S4a) uses the values of the dissociation constants (pK_a) of each of the sulfonamides evaluated [57]. These, in turn, present two values of constants, thus, can be found in solution in three different ways: H_2SF^+ (positive charge, $pH < pK_{a1}$), HSF (neutral charge, $pK_{a1} < pH < pK_{a2}$) and SF^- (negative charge, $pH > pK_{a2}$) (Fig. S4b). Considering that the charges of the protein will also be altered due to the pH of the medium, the nature of the preferred interaction may be different between the ligands depending on the acid-base behavior thereof.

As S1 ($pK_{a1} = 2.06/pK_{a2} = 7.07$) and S4 ($pK_{a1} = 2.46/pK_{a2} = 7.45$) have pK_{a2} close to 7.4 (pH of the medium), these are approximately 50% in its neutral form and 50% in its anionic form allowing the electrostatic interactions to occur. In addition, S1 and S4 are the sulfonamides with less voluminous radicals that end up facilitating the process of interaction through the negative charge of the nitrogen of the sulfonic amide. The sulfonamides S2 ($pK_{a1} = 2.62/pK_{a2} = 6.01$) and S3 ($pK_{a1} = 3.40/pK_{a2} = 5.76$) have $pK_{a2} < 7.4$, they are preferably in anionic form. However, at pH = 7.4, ovalbumin has a negative overall charge (pI = 4.5), so there may be a repulsion between the negative amino acid residues present in OVA (mainly glutamic and aspartic acid) and sulfonamides favoring interaction through Van der Waals forces and hydrogen bonds. These must occur mainly between the protein and the aromatic groups of S2 and S3 or through the oxygen present in the sulfoxide group of these molecules [58,59]. Therefore, the prediction of the affinity between sulfonamides and OVA is not a simple process, due to the number of factors that may affect the interaction process.

3.2. Studies using molecular absorption spectroscopy using UV–vis

To investigate the macromolecule-ligand interactions and alternatively infer about the quenching mechanism involved in the interaction process, UV–vis studies were performed [60]. The molecular absorption spectra of OVA, S1 and OVA-S1 complex were obtained and are shown in Fig. S5a. It can be observed that ovalbumin has a band with maximum absorption peak at 280 nm, characteristic of the aromatic amino acid residues of protein presenting electronic transitions $\pi \rightarrow \pi^*$. The absorption spectrum of the complex formed between OVA and S1 showed a shift towards blue in relation to free OVA, which indicates that the interaction causes conformational changes in the polypeptide chain of the macromolecule [61]. In addition, the absorption spectrum resulting from the subtraction of the supramolecular complex spectrum and the free OVA ($[OVA\text{-}S1]_c$ - OVA) is not overlapping with the free S1 spectrum, confirming that the ground state interaction process occurs [62].

Additionally, according to Tian et al. [63] when the macromolecule-ligand interaction mechanism occurs by dynamic quenching, the UV–vis absorption spectrum of the protein is not altered in the presence of the ligand, as this is caused by collisions between the fluorophore in the excited state in the protein and the ligand. However, when the interaction between the protein and the ligand occurs preferentially by static quenching, changes associated to the formation of the supramolecular complexes in the ground state are observed in the spectrum of absorption by UV–vis (Table S3). These data confirm the results obtained by molecular fluorescence. Similar results were obtained for S2, S3 and S4 and are shown in Fig. S5b–d.

3.3. Evaluation of conformational changes in ovalbumin

3.3.1. Three-dimensional fluorescence (3D)

To evaluate possible conformational changes in the secondary structure of proteins and the microenvironment of their fluorophores (Trp and Tyr) in the presence of the sulfonamides evaluated, a study was carried out using three-dimensional fluorescence [62]. Comprehensive information on OVA fluorescence in the absence and presence of different SA were obtained, and 3D fluorescence spectra for OVA in the absence and presence of S1 are shown in Fig. 2. The OVA spectra in the absence and presence of S2, S3 and S4 are shown in Fig. S6.

The main parameters associated to the 3D spectra obtained regarding the position and intensity of the maximum fluorescence emission and Stokes effect peaks were summarized in Table S4. The fluorescence emission spectra have three main characteristic peaks: (1) related to the Rayleigh scattering of the solvent whenever $\lambda_{ex} = \lambda_{em}$; (2) related to the intrinsic fluorescence of the residues of the Trp and Tyr present in OVA and (3) was attributed to fluorescence from the excitation of higher excited electronic states of the aromatic amino acid residues in the protein [64].

When comparing the free OVA (Fig. 2a) and OVA-S1 (Fig. 2b) graphs, it is possible to observe that in the presence of the sulfonamide there is a decrease in fluorescence relative to peak 2 (52%) and peak 3 (59%) after addition of S1 indicating, therefore, that the secondary structure of the protein was altered in the presence of the ligand and, consequently, the allergic effects of OVA present in eggs from broilers treated with sulfonamides could be potentiated. Similar spectral changes can be observed in the 3D spectra obtained for OVA in the presence of S2, S3 and S4. For S2, peaks 2 and 3 were reduced by 42 and 69%, respectively. For S3 it observed a reduction of 35 and 64%, whereas for S4, of 45 and 71% for peaks 2 and 3, respectively.

3.3.2. Synchronous fluorescence

To monitor separately the Trp and Tyr residues present in OVA, and to verify if alterations in the microenvironment of these amino acids occur in the presence of different SA concentrations, studies were performed based on the synchronous fluorescence technique. Thus, when $\Delta\lambda$ is fixed at 15 and 60 nm, it corresponds to the selective monitoring of the residues of Tyr and Trp, respectively (Fig. 3a) [13].

The spectra referring to OVA titration with S1 when $\Delta\lambda = 15$ and 60 nm are shown in Fig. 3b and c, respectively. As the concentration of S1 increased, there was a reduction in fluorescence intensity for the residues of Tyr and Trp, in addition, red shifts of +21 ($\Delta\lambda = 15$ nm) and + 9 nm ($\Delta\lambda = 60$ nm) relative to the wavelength of maximum emission (Table S5). Additionally, it can be inferred that the microenvironment of these amino acid residues was changed with increasing polarity due to a greater exposure to solvent (water), resulting from the conformational change of OVA in the presence of the ligand [65]. Similar results were obtained for the interaction of OVA with the other SA evaluated and are presented in the supplemental material (Fig. S7).

3.4. Förster resonance energy transfer (FRET)

To measure the distance between the donor (OVA fluorophores) and the receptor (sulfonamides) of energy involved in the interaction process, a study was carried out using FRET [66]. The efficiency of the FRET process depends mainly on the following factors [67]: (i) overlap between the fluorescence emission spectrum of the OVA (donor) and the absorption spectrum of the sulfonamides (receptor) (Fig. S8); (ii) relative orientation of donor and recipient dipoles; (iii) distance (r_0) between the OVA and the energy receptor molecule (1–10 nm).

According to Föster's energy transfer theory, the value of the energy transferred (E) involved in the OVA interaction process with a given

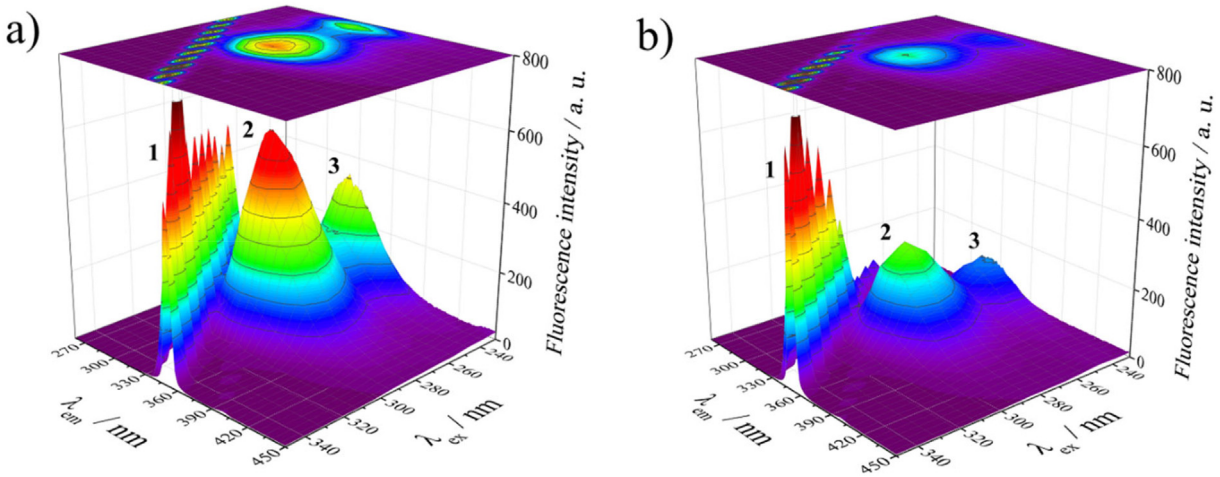


Fig. 2. Three-dimensional (3D) fluorescence spectra for a) OVA, and b) OVA + S1. Conditions: OVA (2 μM), S1 (40 μM), 50 mM Tris-HCl buffer and 100 mM NaCl at pH 7.4 and 30 °C.

sulfonamide is calculated from Eq. (5) [68]:

$$E = 1 - \frac{F}{F_0} = \frac{R_0^6}{R_0^6 + r_0{}^6} \quad (5)$$

in which F and F_0 are the fluorescence intensities of OVA in the presence and absence of SA, respectively, and R_0 is the critical distance when the energy transfer efficiency equals 50%, being calculated from the following equation [68]:

$$R_0^6 = 8.8 \times 10^{-25} K^2 N^{-4} \Phi J \quad (6)$$

being K^2 the spatial orientation factor that describes the geometry of dipoles of the donor and the acceptor of energy ($K^2 = 2/3$ for random alignment), N is the refractive index of the medium ($N = 1.36$), Φ is the quantum yield of the free OVA ($\Phi = 0.118$) and J is the overlap integral of the OVA fluorescence emission spectrum and absorption spectra of the ligands given by [67,69]:

$$J = \frac{\int_0^\infty F(\lambda)\varepsilon(\lambda)\lambda^4 d\lambda}{\int_0^\infty F(\lambda) dy} \quad (7)$$

in which $F(\lambda)$ is the normalized fluorescence intensity of OVA while $\varepsilon(\lambda)$ is the molar absorption coefficient of the SA at wavelength λ. Through the Eqs. (5)–(7) it was possible to obtain the parameters of the FRET study (J, R_0, E and r_0) that are presented in Table 2. The critical Föster distance (R_0) and the distance between the OVA tryptophan residues and the sulfonamides (r_0) are between 1 and 2 nm, indicating that the energy transfer between OVA and sulfonamides occurs with high probability [67]. In addition, it was also observed that for all interaction systems evaluated the energy transfer (E), was <50% and therefore $R_0 < r_0$, agreeing with the results obtained [69].

3.5. Competition study: interaction with the ANS and metal ions

3.5.1. Assay with ANS (8-anilino-1-naphthalenesulfonate)

The organic probe ANS (Fig. S9a) is widely used in protein analysis, since although it has low intrinsic fluorescence in aqueous media, the fluorescence emission intensity increases when the ANS binds in hydrophobic regions of these macromolecules (Fig. S9b) [70]. Thus, ANS was used as a competitor species in the interaction process between OVA and SA, to evaluate if the preferential binding site occurs in hydrophobic regions. For this, the effect of the addition of different concentrations of SA on the OVA-ANS system was evaluated, since if the binding site of the SA in the protein is close to or similar to that of the ANS, a competition will occur, and, in this way, the ligands may affect the fluorescence intensity of the OVA-ANS system [71].

The influence of addition of the different concentrations of SA to the OVA-ANS system is shown in Fig. S9c. When SA is added, the fluorescence emission decreases, however, the reduction is more effective

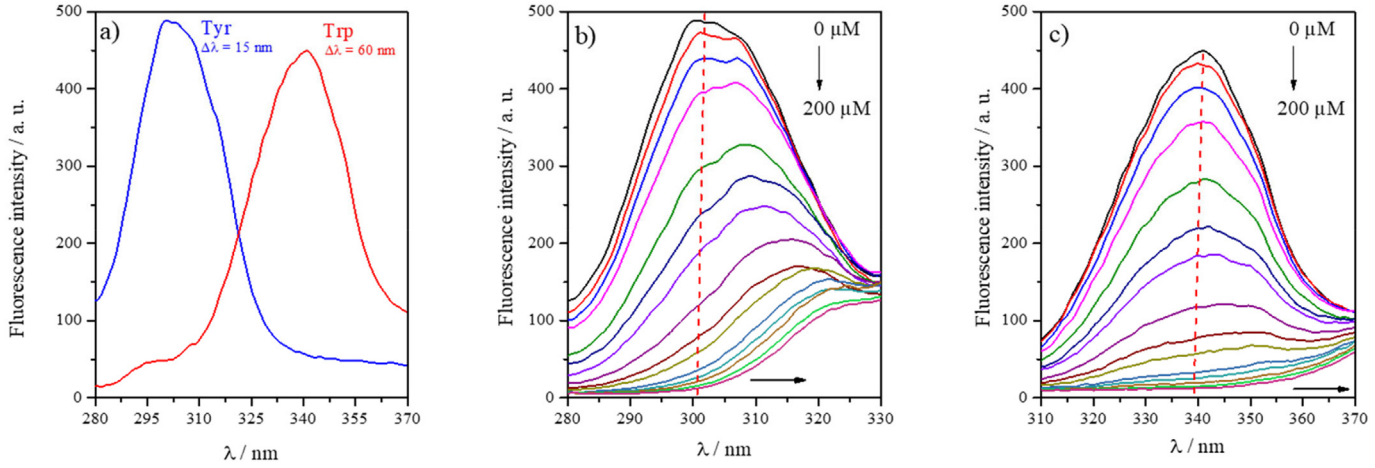


Fig. 3. a) Synchronous emission spectrum for the Tyr residues (Δλ = 15 nm) and Trp (Δλ = 60 nm) of the free OVA. Titration employing synchronous fluorescence for the b) Tyr residue and the c) Trp with addition of S1. Conditions: OVA (2 μM), S1 (0–200 μM), 50 mM Tris-HCl buffer and 100 mM NaCl at pH 7.4 and 30 °C.

t2.1 **Table 2**
t2.2 FRET parameters of the interaction between sulfonamides and OVA.

t2.3 Sulfonamides	J (10^{-16} cm^3 M^{-1})	R_0 (nm)	E (%)	r_0 (nm)
t2.4 S1	2.60	1.32	29.7	1.52
t2.5 S2	13.6	1.74	33.5	1.95
t2.6 S3	1.78	1.24	25.8	1.48
t2.7 S4	3.78	1.40	27.4	1.65

with the addition of sulfaquinoxaline (S2) compared to the other evaluated compounds. According to Guan et al. [61] this indicates that the OVA-S2 interaction process occurs preferentially in hydrophobic sites, since S2 possibly displaces the ANS from the binding region. In addition, this can also be explained by the values of the partition coefficient (logP), which expresses the lipophilicity of organic compounds [72]. For S1, S2, S3 and S4 the logP values were obtained through the program Molinspiration Cheminformatics being equal to 0.83, 1.70, 0.75 and 0.84, respectively. Therefore, knowing that the higher the hydrophobic logP value is the compound, it is verified that S2 is the sulfonamide that has a more hydrophobic molecular structure in relation to the others, thus allowing a greater interaction in hydrophobic regions of OVA. Thus, it is pertinent to infer that the other SA evaluated interact preferentially in more hydrophilic regions, differing from S2.

3.5.2. Competition with metal ions

The objective of this study was to evaluate the influence of metal ions that may be present in the food (Ca(II), Mg(II), Cu(II), Zn(II) and Fe(III)) on the interaction process of the different SA with OVA at pH 7.4 and 30 °C. For this, the ratio between the binding constants in the presence of the competitor ion (K_b') and absence (K_b) was considered as the comparison parameter (Fig. 4). When $K_b'/K_b < 1$ the presence of the ion detracts the formation of the complex OVA-SA, however when $K_b'/K_b > 1$ indicates that the interaction process between the macromolecule and the ligand is favored.

In the Fig. 4 it is shown that the presence of Ca(II), Mg(II) and Fe(III) favored the interaction between OVA with S1 and S2. This may possibly be associated with the conformational change of the protein induced by the binding of these ions to groups (phosphates and thiols, for example) present in their polypeptide chain, and favoring the complex formation [73]. However, Cu(II) and Zn(II) disfavored the formation of these complexes for all SA evaluated, possibility due to the formation of metal complexes between sulfonamides and these cations [74]. Additionally,

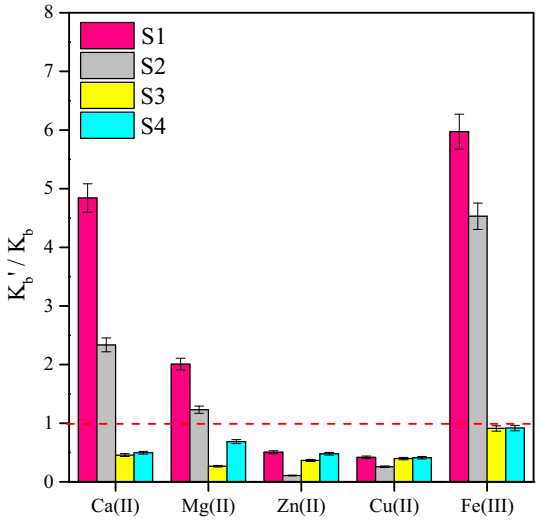


Fig. 4. Effect of the metal ions on the interaction between OVA and sulfonamides. Conditions: Protein and competitors (2 μM), sulfonamides (0–200 μM), 50 mM Tris-HCl buffer and 100 mM NaCl at pH 7.4 and 30 °C.

for S3 and S4 the presence of all the ions has disfavored the interaction with the protein.

3.6. Molecular docking

To get details regarding to interaction mode of sulfonamides into OVA protein we evaluated the main residues within a radius of 6 Å from the most stable protein-sulfonamide complexes obtained from molecular docking simulations. Results of this analysis are showed in Fig. 5. The sulfonamides bind to a very solvent exposed region of OVA protein. Nevertheless, as highlighted in Fig. 5, the main residues involved in each specific interaction between SA molecules and OVA depends of the chemical nature of respective compounds. For instance, the analysis of closest residues in a radius of 6 Å from S1 in S1-OVA complex revealed that the ARG170, VAL172, GLU294, GLU295 and LYS296 residues play an important role on process of interaction of S1 with OVA.

In the other hand, for example in S2-OVA complex, the closest residues around S2 are HIS45, ASN49, TYR138, GLU295, LYS296, ASN298 and SER301. The greatest number of residues contact for S2-OVA complex in relation to S1-OVA is a direct effect of larger molecular size of R (radical) substituent in S2, which is composed by two six membered rings. Overall analysis of the of molecular docking results show that formation of respective SA-OVA complexes is essentially stabilized by a set of hydrogen bonds involving the sulfonyl group and (radical) substituents. To get details with respect to chemical nature of the intermolecular interactions involving the SA molecules and OVA we evaluated the main components of the Gibbs binding free-energy involved in the formation of each complex (Table 3).

In line with experimentally predicted, docking energetic results quoted in Table 3 show that the formation of SA-OVA complexes is a thermodynamically favored process. Worth it highlights that the binding free-energies obtained *via* molecular docking simulations are in very good agreement with experimental values, where the largest deviation between computational and experimental results was ~3.0 kcal mol^{-1} for S1-OVA complex. According to our molecular docking calculations the formation of SA-OVA complexes is governed essentially by nonbonded interactions (van der Waals, hydrogen bonds and desolvation). Regarding to electrostatic interactions, Table 3 shows that these effects are more pronounced in the formation of S1 and S4-OVA complexes. This result is in accordance with thermodynamic values obtained by spectroscopic assay of Table 1 in conjunction with the approach proposed by Hu and co-workers [55].

3.7. Evaluation of the interaction process on the biological activity

To evaluate whether the interaction between OVA and SA interfered or not with the biological action of these antibiotics on different bacteria *in vitro*, a series of antibiograms were performed, with different concentrations of the compounds evaluated in the presence and absence of OVA, and the values of minimal inhibitory concentration (MIC) were determined. The values of the inhibition halos obtained in the preliminary test, using 100 and 50 μg dosages of SA and their combinations, are shown in Table S6 (supplementary material).

According to the parameters established by the Institute of Clinical and Laboratory Standards [43], for a microorganism to be sensitive to the SA class, the inhibition halo values should be ≥17 mm. However, it was observed in the preliminary assay that only *E. coli* (Gram negative bacilli) and *B. megaterium* (Gram positive bacilli) were sensitive in the SA concentrations tested (Fig. 6a). The other bacteria tested were resistant to such antibiotics (inhibition halos ≤12 mm) and to systems containing antibiotic and OVA. Therefore, relative tests to establish MIC values were performed only against *E. coli* and *B. megaterium.*

To determine MIC values, the dosages tested ranged from 0.125 to 50 μg (S1, S2 and S4) and from 0.05 to 25 μg (S3). The results obtained for sulfathiazole (S1) are shown in Fig. 6b and c, it being observed that, as

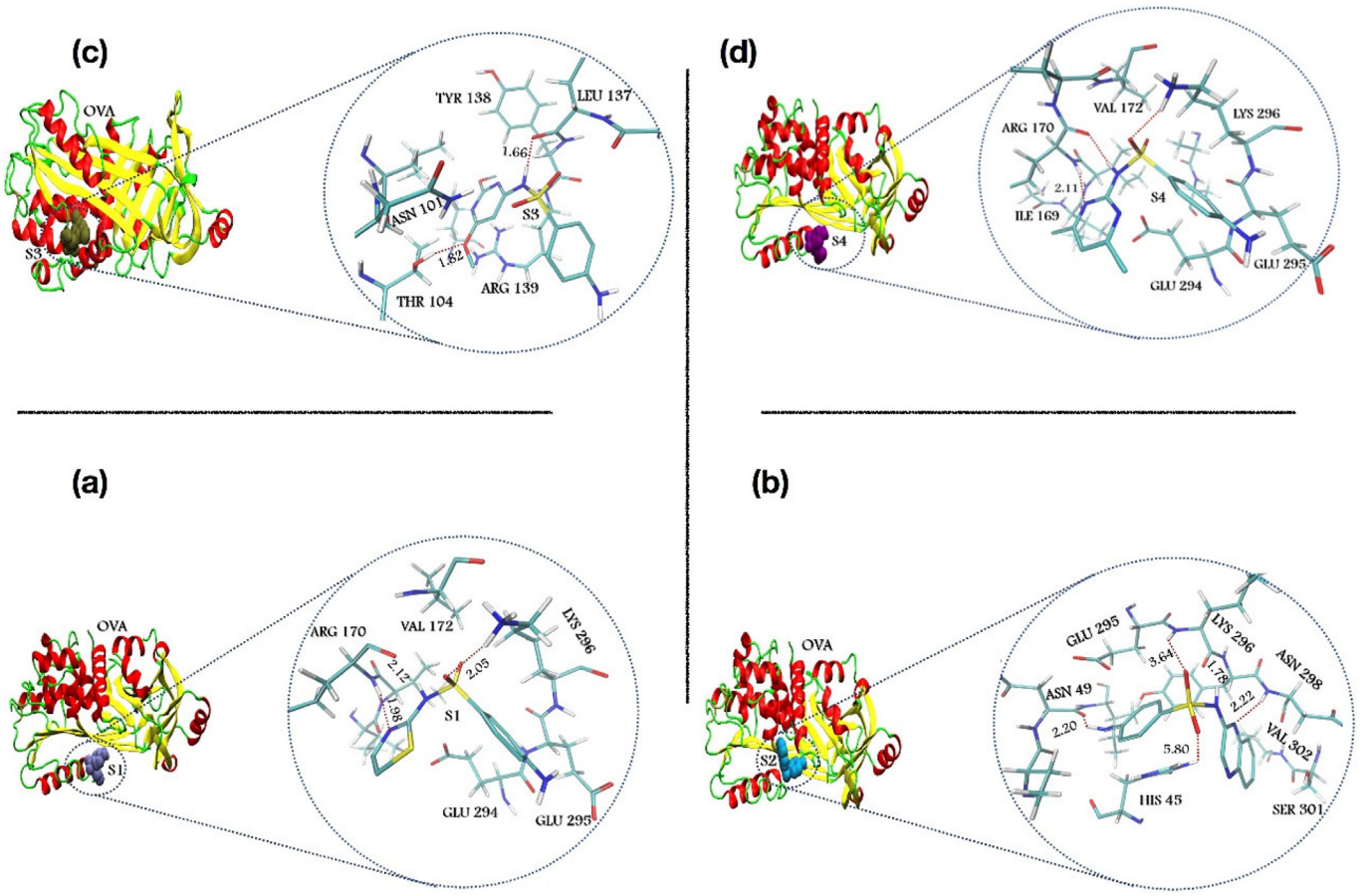


Fig. 5. Preferential bind region of SA molecules in OVA protein predicted by molecular docking simulations after complex formation, (a) OVA—S1, (b) OVA—S2, (c) OVA-S3 and (d) S4-OVA. In zoom are showed the residues in a radius of 6 Å measured from SA molecules.

dosages decreased, smaller inhibition halos were obtained. In general, the inhibition halos for antimicrobial activity of free S1 are lower when compared to the halos obtained for the S1-OVA systems (with only 50% concentration). MIC values in the absence and presence of OVA did not vary independently of the evaluated bacteria, however, change the inhibition activity profile was observed since systematically the halos values of SA are lower in the presence of protein. Thus, the MIC found for S1 was the one obtained with the dosage equal to 2.5 μg for *E. coli* and 25 μg for *B. megaterium*, because at lower dosages the halos were smaller than 17 mm. Similar results were obtained for the remaining SA and are shown in Figs. S10 and S11 (supplementary material). For S2, S3 and S4 the MIC against *E. coli* were obtained at the dosages of 1.0; 2.5 and 25 μg, respectively, while against *B. megaterium*, the MIC were obtained at the dosages of 25 μg for all the tested SA. The antibiograms of S1 against *E. coli* and *B. megaterium*, respectively at the dosages of 2.5 and 0.125 μg, are shown in Figs. S12 and S13 (supplementary material).

According to studies of Argyropoulou et al. [75], the MIC of sulfamethoxazole against *B. megaterium* BGSC 7A2 and *E. coli* SPA27 was higher than 1.5 μg mL^{-1} (around 0.030 μg) and 100 μg mL^{-1} (around 2 μg), respectively. These MICs were lower than the ones obtained in the present study for sulphathiazole (S1), for instance, it means, *ca.* 0.125 μg and 2.5 for the strains *E. coli* ATCC 25922 and *B. megaterium* APFSG3isox respectively, and they were still more improved by the combination with trimethoprim – a competitive inhibitor of the dihydrofolate reductase (the enzyme that reduce dihydrofolate to tetrahydrofolate). In our study, the combination OVA-SA did not affect the antimicrobial activity of the SA, but change the inhibition activity profile.

t3.1 **Table 3**
t3.2 Gibbs binding free-energy calculated for the formation of SA-OVA complexes.

t3.3 Compound	ΔG_{exp} (kcal mol^{-1})	$\Delta G_{binding}$ (kcal mol^{-1})	vdW + H-bond+desolv (kcal mol^{-1})	Electrostatic energy (kcal mol^{-1})
t3.4 S1	−8.80	−6.00	−6.95	−0.22
t3.5 S2	−7.90	−6.40	−7.40	−0.17
t3.6 S3	−7.74	−5.70	−7.30	−0.20
t3.7 S4	−7.70	−7.00	−7.03	−1.16

4. Conclusion

The interaction process between OVA and SA was investigated by molecular fluorescence, UV–vis, theoretical studies and biological assays. The formation of supramolecular complexes, OVA-SA, occurred with high affinity, and sulfatiazol (S1) presented the highest interaction constant with commercial or *in natura* OVA. Modifications in the polypeptide chain of OVA were verified by synchronous fluorescence and 3D, which can enhance the natural allergenicity characteristics of OVA, posing a risk in human food safety. Competition studies indicate that sulfonamide S2 interacts preferentially at hydrophobic sites of the protein and that Ca(II), Mg(II) and Fe(III) potentiate the interaction process of OVA with S1 and S2. Molecular docking simulations predicted that the sulfonamides bind to a very solvent exposed region of OVA protein, where the formation of respective SA-OVA complexes is essentially stabilized by a set of hydrogen bonds involving the sulfonyl group and R substituents. The binding free-energy calculated by molecular docking showed a very good agreement with the experimental measurements. Finally, biological studies show that the interaction between SA and OVA do not affect the antimicrobial activity of these antibiotics (MIC

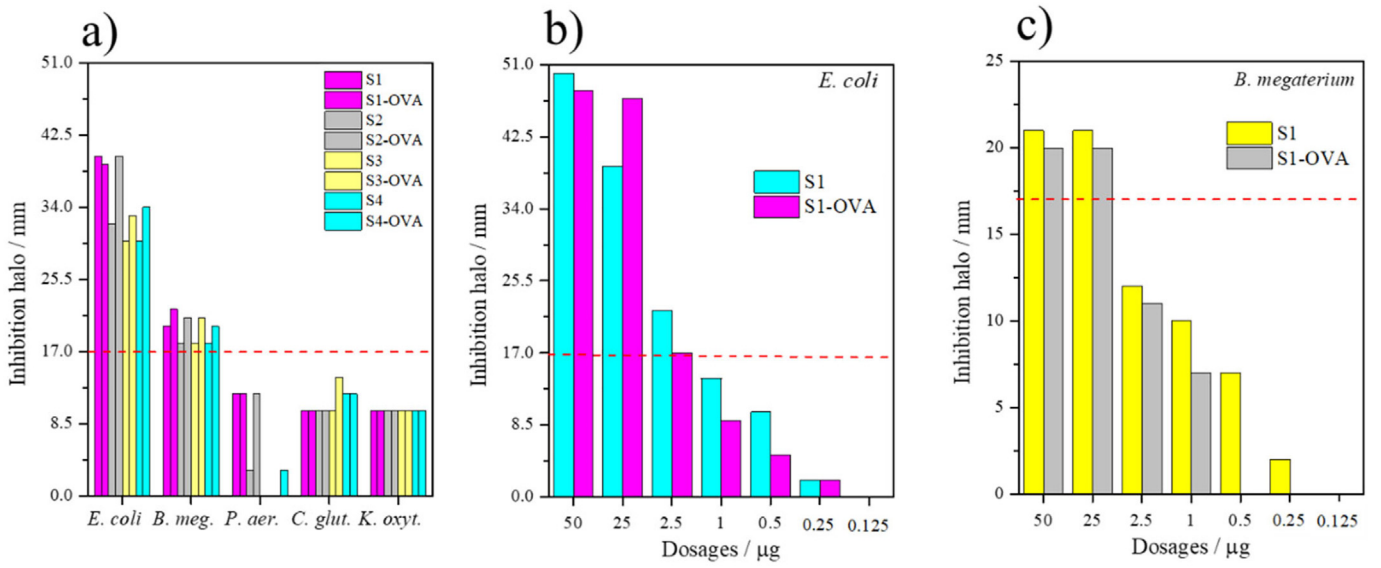


Fig. 6. Effect *(in vitro* inhibition halos) of sulfonamides (a) on all bacterial strains tested (*Escherichia coli* ATCC 25922, *Pseudomonas aeruginosa* ATCC 27853, *Corynebacterium glutamicum* LBPMA, *Klebsiella oxytoca* BMA-13 and *Bacillus megaterium* APFSG3isox) and different dosages of sulfathiazole (S1) against (b) *E. coli* ATCC 25922 and c) *B. megaterium* APFSG3isox.

values) against strains of *E. coli* and *B. megaterium*, however, change the inhibition activity profile.

Declaration of competing interests

The authors declare that they have no known competing financial interests or personal relationships that could have appeared to influence the work reported in this paper.

Acknowledgements

We thank the IQB-PPGQB, FAPEAL (Fundação de Amparo à Pesquisa do Estado de Alagoas), and CNPq (Conselho Nacional de Desenvolvimento Científico e Tecnológico) for financial support and fellowships. This study was financed in part by the Coordenação de Aperfeiçoamento de Pessoal de Nível Superior - Brazil (CAPES) - Finance Code 001.

Appendix A. Supplementary data

Supplementary data to this article can be found online at https://doi.org/10.1016/j.saa.2019.117747.

References

[1] A.C.C. Alleoni, Albumen protein and functional properties of gelation and foaming, Sci. Agric. 63 (3) (2006) 291–298.
[2] M. Bhattacharya, S. Mukhopadhyay, Structural and dynamical insights into the molten-globule form of ovalbumin, J. Phys. Chem. B 116 (2012) 520–531.
[3] Y. Hu, H. Liang, W. Xu, Y. Wang, Y. An, X. Yan, S. Ye, Q. Huang, J. Liu, B. Li, Synergistic effects of small amounts of konjac glucomannan on functional properties of egg white protein, Food Hydrocoll. 52 (2016) 213–220.
[4] Y. Mine, Egg proteins and peptides in human health-chemistry, bioactivity and production, Curr. Pharm. Des. 13 (2007) 875–884.
[5] J.-C. Caubet, J. Wang, Current understanding of egg allergy, Pediatr. Clin. N. Am. 58 (2) (2011) 427–443.
[6] J.B. Ulmer, U. Valley, R. Rappuoli, Vaccine manufacturing: challenges and solutions, Nat. Biotechnol. 24 (11) (2006) 1377–1383.
[7] E.H. Chung, Clinical and experimental vaccine research, Clin. Exp. Vaccine Res. 3 (2014) 50–57.
[8] K.C.M. Verhoeckx, Y.M. Vissers, J.L. Baumert, R. Faludi, M. Feys, S. Flanagan, C. Herouet-Guicheney, T. Holzhauser, R. Shimojo, N.V.D. Bolt, H. Wichers, I. Kimber, Food processing and allergenicity, Food Chem. Toxicol. 80 (2015) 223–240.
[9] Y. Mine, P. Rupa, Fine mapping and structural analysis of immunodominant IgE allergenic epitopes in chicken egg ovalbumin, Protein Eng. 16 (10) (2003) 747–752.
[10] J. Wang, H.A. Sampson, Food allergy: recent advances in pathophysiology and treatment, Allergy, Asthma Immunol. Res. 1 (1) (2009) 19–29.
[11] T. Kamilya, P. Pal, G.B. Talapatra, Interaction of ovalbumin with phospholipids langmuir-Blodgett film, J. Phys. Chem. B 111 (2007) 1199–1205.
[12] Y. Lu, Y.-L. Wang, S.-H. Gao, G.-K. Wang, C.-L. Yan, D.-J. Chen, Interaction of quercetin with ovalbumin: spectroscopic and molecular modeling studies, J. Lumin. 129 (2009) 1048–1054.
[13] R. Wang, Y. Yin, H. Li, Y. Wang, J.-J. Pu, R. Wang, H. Dou, C. Song, R. Wang, Comparative study of the interactions between ovalbumin and three alkaloids by spectrofluorimetry, Mol. Biol. Rep. 40 (2013) 3409–3418.
[14] F. Shen, F. Niu, J. Li, Y. Su, Y. Liu, Y. Yang, Interactions between tea polyphenol and two kinds of typical egg white proteins – ovalbumin and lysozyme: effect on the gastrointestinal digestion of both proteins *in vitro*, Food Res. Int. 59 (2014) 100–107.
[15] J. Ognjenovic, M. Stojadinovic, M. Milcic, D. Apostolovic, J. Vesic, I. Stambolic, M. Atanaskovic-Markovic, M. Simonovic, T.C. Velickovic, Interactions of epigallocatechin 3-gallate and ovalbumin, the major allergen of egg white, Food Chem. 164 (2014) 36–43.
[16] P. Manivel, M. Parthiban, M. Ilanchelian, Exploring the binding mechanism between methylene blue and ovalbumin using spectroscopic analyses and computational simulations, J. Biomol. Struct. Dyn. 4 (2019) 1–10.
[17] R. Rajamanikandan, A.S. Sharma, M. Ilanchelian, New insights into the binding interaction of food protein ovalbumin with malachite green dye by hybrid spectroscopic and molecular docking analysis, J. Biomol. Struct. Dyn. 19 (2019) 1–12.
[18] Z. Ma, G. Prasanna, L. Jiang, P. Jing, Molecular interaction of cyanidin-3-O-glucoside with ovalbumin: insights from spectroscopic, molecular docking and in vitro digestive studies, J. Biomol. Struct. Dyn. 23 (2019) 1–10.
[19] R. Hoff, T.B.L. Kist, Analysis of sulfonamides by capillary electrophoresis, J. Sep. Sci. 32 (2009) 854–866.
[20] E. Pacheco-Silva, J.R. Souza, E.D. Caldas, Veterinary drug residues in milk and eggs, Quim Nova 37 (1) (2014) 111–122.
[21] M.D. Mund, U.H. Khan, U. Tahir, Bahar-E-Mustafa, A. Fayyaz, Antimicrobial drug residues in poultry products and implications on public health: a review, Int. J. Food Prop. 20 (7) (2017) 1433–1446.
[22] A. Mehtabuddin, A. Mian, T. Ahmad, S. Nadeem, Z.I. Tanveer, J. Arshad, Sulfonamide residues determination in commercial poultry meat and eggs, J. Anim. Plant Sci. 22 (2) (2012) 473–478.
[23] Y. Xu, J. Ding, H. Chen, Q. Zhao, J. Hou, J. Yan, H. Wang, L. Ding, N. Ren, Fast determination of sulfonamides from egg samples using magnetic multiwalled carbon nanotubes as adsorbents followed by liquid chromatography-tandem mass spectrometry, Food Chem. 140 (2013) 83–90.
[24] A.D. Bani-yanseen, Spectrofluorimetric study on the interaction between antimicrobial drug sulfamethazine and bovine serum albumin, J. Lumin. 131 (2011) 1042–1047.
[25] J. Chen, X. Zhou, Y. Zhang, H. Gao, Potential toxicity of sulfanilamide antibiotic: binding of sulfamethazine to human serum albumin, Sci. Total Environ. 432 (2012) 269–274.
[26] M.S. Ali, H.A. Al-Lohedan, Interaction of human serum albumin with sulfadiazine, J. Mol. Liq. 197 (2014) 124–130.
[27] Q. Wang, Zhang Sheng-Rui, X. Ji, Investigation of interaction of antibacterial drug sulfamethoxazole with human serum albumin by molecular modeling and multi-spectroscopic method, Spectrochim. Acta, Part A 124 (2014) 84–90.
[28] W. He, H. Dou, Z. Li, X. Wang, L. Wang, R. Wang, J. Chang, Investigation of the interaction between five alkaloids and human hemoglobin by fluorescence spectroscopy and molecular modeling, Spectrochim. Acta, Part A 123 (2014) 176–186.
[29] A. Varlan, M. Hillebrand, Bovine and human serum albumin interactions with 3-carboxyphenoxathiin studied by fluorescence and circular dichroism spectroscopy, Molecules 15 (2010) 3905–3919.

ARTICLE IN PRESS

[30] T. Chatterjee, A. Pal, S. Dey, B.K. Chatterjee, P. Chakrabarti, Interaction of virstatin with human serum albumin: spectroscopic analysis and molecular modeling, PLoS One 7 (5) (2012).

[31] C. Lee, W. Yang, R.G. Parr, Development of the Colle-Salvetti correlation energy formula into a functional of the electron density, Phys. Rev. B.: Condes. Matter Mater. Phys. 37 (1988) 785–789.

[32] A.D. Becke, Density functional thermochemistry. III. The role of exact exchange, J. Chem. Phys. 98 (1993) 5648–5652.

[33] R. Ditchfield, W.J. Hehre, J.A. Pople, Self-consistent molecular-orbital methods. IX. An extended Gaussian-type basis for molecular-orbital studies of organic molecules, J. Chem. Phys. 54 (1971) 724–728.

[34] M.J. Frisch, G.W. Trucks, H.B. Schlegel, G.E. Scuseria, M.A. Robb, J.R. Cheeseman, G. Scalmani, V. Barone, B. Mennucci, G.A. Petersson, H. Nakatsuji, M. Caricato, X. Li, H.P. Hratchian, A.F. Izmaylov, J. Bloino, G. Zheng, J.L. Sonnenberg, M. Hada, M. Ehara, K. Toyota, R. Fukuda, J. Hasegawa, M. Ishida, T. Nakajima, Y. Honda, O. Kitao, H. Nakai, T. Vreven, J.A. Montgomery Jr., J.E. Peralta, F. Ogliaro, M. Bearpark, J.J. Heyd, E. Brothers, K.N. Kudin, V.N. Staroverov, R. Kobayashi, J. Normand, K. Raghavachari, A. Rendell, J.C. Burant, S.S. Iyengar, J. Tomasi, M. Cossi, N. Rega, J.M. Millam, M. Klene, J.E. Knox, J.B. Cross, V. Bakken, C. Adamo, J. Jaramillo, R. Gomperts, R.E. Stratmann, O. Yazyev, A.J. Austin, R. Cammi, C. Pomelli, J.W. Ochterski, R.L. Martin, K. Morokuma, V.G. Zakrzewski, G.A. Voth, P. Salvador, J.J. Dannenberg, S. Dapprich, A.D. Daniels, Ö. Farkas, J.B. Foresman, J.V. Ortiz, J. Cioslowski, D.J. Fox, Gaussian 09, Revision C.01, Gaussian, Inc, Wallingford CT, 2009.

[35] G.M. Morris, D.S. Goodsell, R.S. Halliday, R. Huey, W.E. Hart, R.K. Belew, A.J. Olson, Automated docking using a Lamarckian genetic algorithm and an empirical binding free energy function, J. Comput. Chem. 19 (1998) 1639–1662.

[36] G.M. Morris, R. Huey, W. Lindstrom, M.F. Sanner, R.K. Belew, D.S. Goodsell, A.J. Olson, AutoDock4 and AutoDockTools4: automated docking with selective receptor flexibility, J. Comput. Chem. 30 (2009) 2785–2791.

[37] M.F. Sanner, Python: a programming language for software integration and development, J. Mol. Graph. Model. 17 (1999) 57–61.

[38] J. Gasteiger, M. Marsili, A new model for calculating atomic charges in molecules, Tetrahedron Lett. 19 (1978) 3181–3184.

[39] J. Gasteiger, M. Marsili, Iterative partial equalization of orbital electronegativity: a rapid access to atomic charges, Tetrahedron 36 (1980) 3219–3228.

[40] T.A. Soares, D.S. Goodsell, R. Ferreira, A.J. Olson, J.M. Briggs, Ionization state and molecular docking studies for the macrophage migration inhibitory factor: the role of lysine 32 in the catalytic mechanism, J. Mol. Recognit. 13 (2000) 146–156.

[41] X.-Y. Meng, H.-X. Zhang, M. Mezei, M. Cui, Molecular docking: a powerful approach for structure-based drug discovery, Curr. Comp. Aid Drug Des. 7 (2011) 146–157.

[42] Z. Dolatkhah, S. Javanshir, A.S. Sadr, J. Hosseini, S. Sardori, Synthesis, molecular docking, molecular dynamics studies, and biological evaluation of 4H-chromone-1,2,3,4-tetrahydropyrimidine-5-carboxylate derivatives as potential antileukemic agents, J. Chem. Inf. Model. 57 (2017) 1246–1257.

[43] CLSI (Clinical and Laboratory Standards Institute), Performance standards for antimicrobial disk susceptibility testing, http://www.facm.ucl.ac.be/intranet/CLSI/CLSI-M100S17-susceptibility-testing-2007-unlocked.pdf 2007 (accessed at June 26, 2018).

[44] A.W. Bauer, W.M. Kirby, J.C. Sherris, M. Turck, Antibiotic susceptibility testing by a standardized single disk method, Am. J. Clin. Pathol. 45 (4) (1966) 493–496.

[45] L. Sheng, M. Huang, J. Wang, Q. Xu, H.H.A. Hammad, M. Ma, A study of storage impact on ovalbumin structure of chicken egg, J. Food Eng. 219 (2018) 1–7.

[46] Y. Ni, S. Wang, S. Kokot, Spectrometric study of the interaction between alpinetin and bovine serum albumin using chemometrics approaches, Anal. Chim. Acta 663 (2010) 139–146.

[47] X. He, Z. Song, Study on the proteins-luminol biding by use of luminal as a fluorescence probe, Spectrochim. Acta, Part A 114 (2013) 231–235.

[48] T.A. Wani, A.H. Bakheit, S. Zargar, M.A. Hamidaddin, I.A. Darwish, Spectrophotometric and molecular modeling studies on *in vitro* interaction of tyrosine kinase inhibitor linifanib with bovine serum albumin, PLoS One 12 (4) (2017) 1–12.

[49] P. Mei, Li-Xia Zhang, Y. Liu, Li-Hua Cai, Pei-Zhi Hu, Fluorescence quenching study on the interaction of some Schiff base complexes with bovine serum albumin, Chin. J. Chem. 26 (2008) 85–91.

[50] T.C.A. Lage, T.M.S. Maciel, Y.C.C. Mota, F. Sisto, J.R. Sabino, J.C.C. Santos, I.M. Figueiredo, C. Masia, A. de Fátima, S.A. Fernandes, L.V. Modolo, *In vitro* inhibition of *Helicobacter pylori* and interaction studies of lichen natural products with jack bean urease, New J. Chem. 42 (2018) 5356–5366.

[51] M.D.A. Dantas, H.A. Tenório, T.I.B. Lopes, H.J.V. Pereira, A.J. Marsaioli, I.M. Figueiredo, J.C.C. Santos, Interactions of tetracyclines with ovalbumin, the main allergen protein from egg white: spectroscopic and electrophoretic studies, Int. J. Biol. Macromol. 102 (2017) 505–514.

[52] A. Mathavan, A. Ramdass, S. Rajagopal, A spectroscopy approach for the study of the interaction of oxovanadium(IV)-salen complexes with proteins, J. Fluoresc. 25 (2015) 1141–1149.

[53] S.F. Koly, S.P. Kundu, S. Kabir, M.S. Amran, M.Z. Sultan, Analysis of aceclofenac and bovine serum albumin interaction using fluorescence quenching method for predictive, preventive, and personalized medicine, EPMA Journal 6 (24) (2015).

[54] O.A. Chaves, A.P.O. Amorim, L.H.E. Castro, C.M.R. Sant'Anna, M.C.C. Oliveira, D. Cesarin-Sobrinho, J.C. Netto-Ferreira, A.B.B. Ferreira, Fluorescence and docking studies of the interaction between human serum albumin and pheophytin, Molecules 20 (2015) 19526–19539.

[55] Y.-J. Hu, Y. Liu, Ru-Ming Zhao, Jia-Xin Donga, Qu Song-Sheng, Spectroscopic studies on the interaction between methylene blue and bovine serum albumin, J. Photochem. Photobiol., A 179 (2006) 324–329.

[56] J.C.N. Santos, I.M. da Silva, T.C. Braga, A. de Fátima, I.M. Figueiredo, J.C.C. Santos, Thimerosal changes protein conformation and increase the rate of fibrillation in physiological conditions: spectroscopic studies using bovine serum albumin (BSA), Int. J. Biol. Macromol. 113 (1) (2018) 1032–1040.

[57] A. Kaufmann, S. Roth, B. Ryser, M. Widmer, Quantitative LC/MS-MS determination of sulfonamides and some other antibiotics in honey, J. AOAC Int. 85 (2002) 1–8.

[58] A.D. Nisbet, R.H. Saundry, A.J.G. Moir, L.A. Fothergill, J.E. Fothergill, The complete amino-acid sequence of hen ovalbumin, Eur. J. Biochem. 115 (1981) 335–345.

[59] E.D.N.S. Abeyrathne, H.Y. Lee, D.U. Ahn, Sequential separation of lysozyme, ovomucin, ovotransferrin, and ovalbumin from egg white, Poult. Sci. 93 (2014) 1001–1009.

[60] L.-L. He, Z.-X. Wang, Y.-X. Wang, X.-P. Liu, Y.-J. Yang, Y.-P. Gao, X. Wang, B. Liu, X. Wang, Studies on the interaction between promethazine and human serum albumin in the presence of flavonoids by spectroscopic and molecular modeling techniques, Colloids Surface B 145 (2016) 820–829.

[61] Y. Guan, H. Zhang, Y. Wang, New insight into the binding interaction of hydroxylated carbon nanotubes with bovine serum albumin, Spectrochim. Acta, Part A 124 (2014) 556–563.

[62] M. Saeidifar, H. Mansouri-torshizi, A.A. Saboury, Biophysical study on the interaction between two palladium (II) complexes and human serum albumin by multispectroscopic methods, J. Lumin. 167 (2015) 391–398.

[63] Fang-Fang Tian, Feng-Lei Jiang, Xiao-Len Han, C. Xiang, Yu-Shu Ge, Jia-Han Li, Y. Zhang, R. Li, Xin-Liang Ding, Y. Liu, Synthesis of a novel hydrazone derivative and biophysical studies of its interactions with bovine serum albumin by spectroscopic, electrochemical, and molecular docking methods, J. Phys. Chem. B 114 (2010) 14842–14853.

[64] S. Das, S. Pahari, S. Sarmah, M.A. Rohman, D. Paul, M. Jana, A.S. Roy, Lysozyme-luteolin binding: molecular insights into the complexation process and the inhibitory effects of luteolin towards protein modification, Phys. Chem. Chem. Phys. 21 (2019) 12649–12666.

[65] R. Han, B. Liu, G. Li, Q. Zhang, Investigation on the interaction of cefpirome sulfate with lysozyme by fluorescence quenching spectroscopy and synchronous fluorescence spectroscopy, Luminescence 31 (2016) 580–586.

[66] P.N. Naik, S.A. Chimatadar, S.T. Nandibwoor, Interaction between a potent corticosteroid drug – dexamethasone with bovine serum albumin and human serum albumin: a fluorescence quenching and fourier transformation infrared spectroscopy study, J. Photochem. Photobiol. B 100 (2010) 147–159.

[67] Z. Hongwei, G. Min, Z. Zhaoxia, W. Wenfeng, W. Guozhong, Spectroscopic studies on the interaction between riboflavin and albumins, Spectrochim. Acta, Part A 65 (2006) 811–817.

[68] S. Ranjbar, Y. Shokoohinia, S. Ghobadi, N. Bijari, S. Gholamzadeh, N. Moradi, M.R. Ashrafi-Kooshk, A. Aghaei, R. Khodarahmi1, Studies of the interaction between isoimperatorin and human serum albumin by multispectroscopic method: identification of possible binding site of the compound using esterase activity of the protein, Sci. World J. 2013 (2013) 1–13.

[69] M. Sarkar, S.S. Paul, K.K. Mukherjea, Interaction of bovine serum albumin with apsychotropic drug alprazolam: physicochemical, photophysical and molecular docking studies, J. Lumin. 142 (2013) 220–230.

[70] E. Schönbrunn, S. Eschenburg, K. Luger, W. Kabsch, N. Amrheini, Structural basis for the interaction of the fluorescence probe 8-anilino-1 naphthalene sulfonate (ANS) with the antibiotic target MurA, PNAS 97 (12) (2000) 6345–6349.

[71] W.J. Andrews, C.A. Bradley, E. Hamilton, C. Daly, T. Mallon, D.J. Timson, A calcium-dependent interaction between calmodulin and the calponin homology domain of human IQGAP1, Mol. Cell. Biochem. 371 (2012) 217–223.

[72] W.M. Meylan, P.H. Howard, Atom/fragment contribution method for estimating octanol-water partition coefficients, J. Pharm. Sci. 84 (1) (1995) 83–92.

[73] Y. Yang, D. Li, C. Xu, Influences of urea, pH and metal ions on the interaction between cepharanthine and lysozyme by steady state fluorescence spectroscopy, J. Mol. Struct. 1084 (2015) 229–235.

[74] D.P. Rocha, G.F. Pinto, R. Ruggiero, C.A. Oliveira, W. Guerra, A.P.S. Fontes, T.T. Tavares, I.M. Marzano, E.C. Pereira-Maia, Coordination of metals to antibiotics as a strategy to combat bacterial resistance, Quim Nova 34 (1) (2011) 111–118.

[75] I. Argyropoulou, A. Geronikaki, P. Vicini, F. Zani, Synthesis and biological evaluation of sulfonamide thiazole and benzothiazole derivatives as antimicrobial agents, Arkivoc 6 (2009) 89–102.

SUPPLEMENTARY MATERIAL

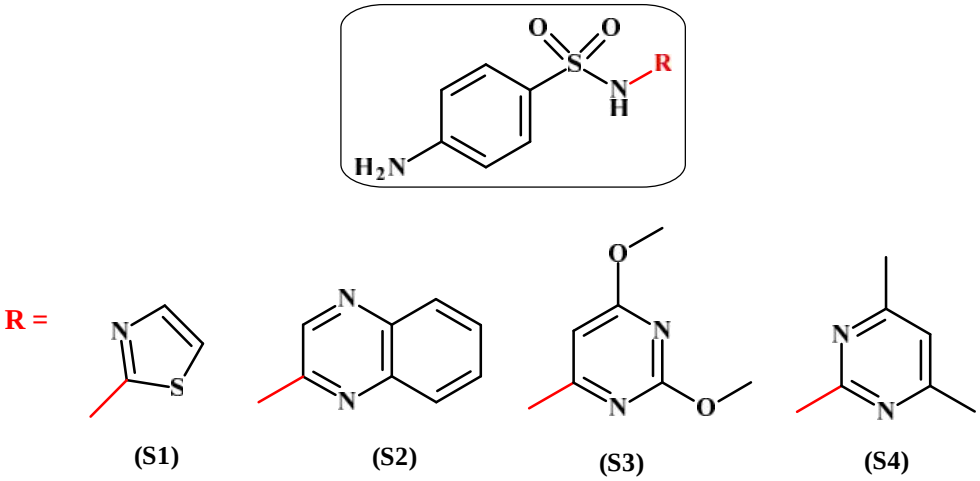
Molecular interaction of sulfonamides and ovalbumin, an allergenic egg protein, exploring biophysical, theoretical and biological studies

Ana Carolina F. de Lyra, Amanda L. dos Santos Silva, Elane Cristina L. dos Santos, Ana Maria Queijeiro López, Júlio Cosme S. da Silva, Isis M. Figueiredo, Josué Carinhanha Caldas Santos✉

Institute of Chemistry and Biotechnology, Federal University of Alagoas, Campus A. C. Simões, 57072-900, Maceió, Alagoas, Brazil.

✉ Corresponding author (JCCS)
E-mail: josue@iqb.ufal.br // jcarinhanha@yahoo.com.br

Introduction



Scheme 1. Sulfonamides evaluated in the interaction process with the allergenic protein ovalbumin: sulfathiazole (S1), sulfaquinoxaline (S2), sulfadimetoxin (S3) and sulfametazine (S4).

Results and Discussion

Binding and thermodynamic parameters associated with the interaction process.

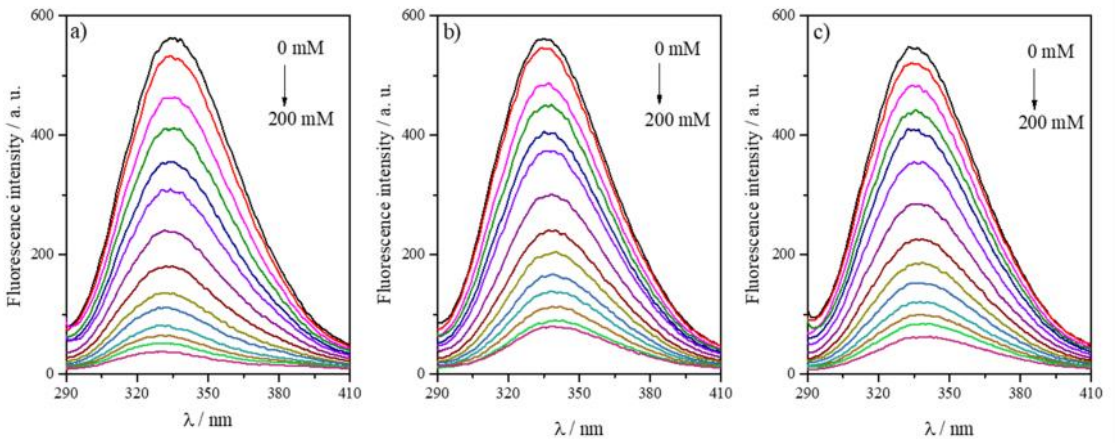


Fig. S1. Spectrofluorometric titration of ovalbumin with the sulfonamides: a) sulfaquinoxaline (S2), b) sulfadimethoxine (S3) and c) sulfamethazine (S4). Conditions: OVA (2 mM), sulfonamides (0-200 μM), 50 mM Tris-HCl buffer and 100 mM NaCl at pH 7.4 and 30ºC.

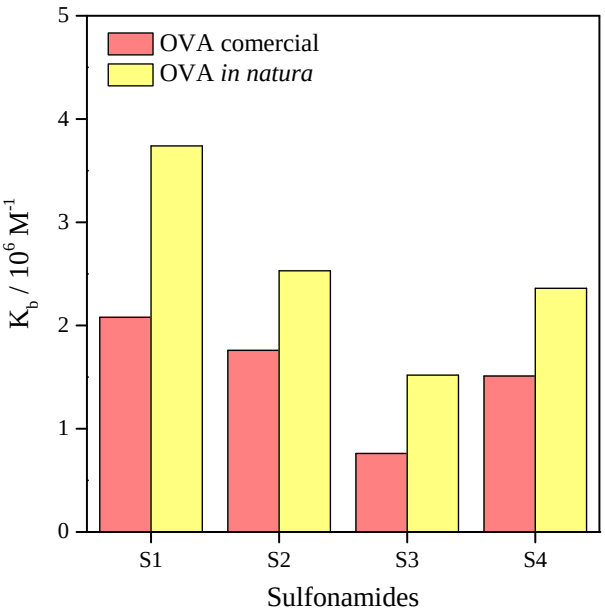


Fig. S2. Comparison of binding constants (K_b) of the process of interaction of sulfonamides with commercial and *in natura* OVA. Conditions: commercial and *in natura* protein (2 μM), sulfonamides (0-200 μM), 50 mM Tris-HCl buffer and 100 mM NaCl at pH 7.4 and 30ºC.

Table S1
Comparison of K_b values of different proteins and sulfonamides with the proposed work.

Buffer	pH	Protein	C_P (μM)	T (ºC)	Compound	K_b ($\times 10^5$ M^{-1})	References
Phosphate (1 mM)	7.4	BSA	2.0	31	Sulfamethazine	3.24	[1]
Tris-HCl 5 mM com NaCl 50 mM	7.4	HSA	1.0	26	Sulfasalazine	2.31	[2]
Sodium phosphate*	7.4	HSA	3.8	30	Sulfamethazine	0.15	[3]
Sodium phosphate*	7.4	HSA	1.5	30	Sulfadiazine	0.02	[4]
Tris-HCl 50 mM and NaCl 100 mM	7.4	HSA	3.0	30	Sulfamethoxazole	0.03	[5]
Tris-HCl (0.02 mM)	7.4	BSA	20	27	Sulfanilamide	0.06	[6]
					Sulfamethoxazole	0.09	
Tris-HCl 50 mM com NaCl 100 mM	7.4	OVA	2.0	30	Sulfathiazole	27.7	This study
					Sulfaquinoxaline	5.17	
					Sulfadimethoxine	3.98	
					Sulfamethazine	4.14	

Note: C_P = concentration of protein / *value of the concentration not informed.

Table S2
Comparison of K_b values of ovalbumin with different ligands with the proposed work.

Buffer	pH	C_P (μM)	T (ºC)	Ligand	K_b ($\times 10^5$ M^{-1})	References
Tris-HCl 100 mM and NaCl 100 mM	7.4	10	27	Quercetin	3.33	[7]
Tris-HCl 100 mM and NaCl 80 mM	7.4	30	24	Diprofylline	0.17	[8]
				Caffeine	0.11	
				Theophylline	0.04	
Sodium phosphate	7.5	-*	-*	Green tea polyphenols	0.08	[9]
Tris-HCl 20 mM	7.0	22	60	Acrylamide	3.37	[10]
Tris-HCl 50 mM and NaCl 100 mM	7.4	2.0	30	Tetracycline	0.27	[11]
Sodium phosphate	7.4	4.99	25	Methylene blue	3.53	[12]
Sodium phosphate	7.4	5.00	25	Malachite green	3.63	[13]
Sodium phosphate	7.0	10	25	Cyanidin-3-O-glucoside	7.54	[14]
Tris-HCl 50 mM and NaCl 100 mM	7.4	2.0	30	Sulfathiazole	27.7	This study
				Sulfaquinoxaline	5.17	
				Sulfadimethoxine	3.98	
				Sulfamethazine	4.14	

Note: C_P = concentration of protein / *values of the concentration and temperature not informed.

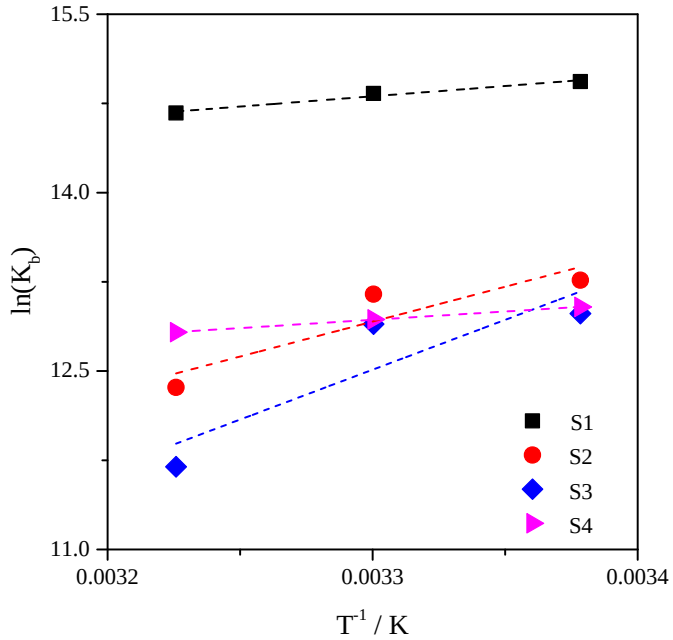
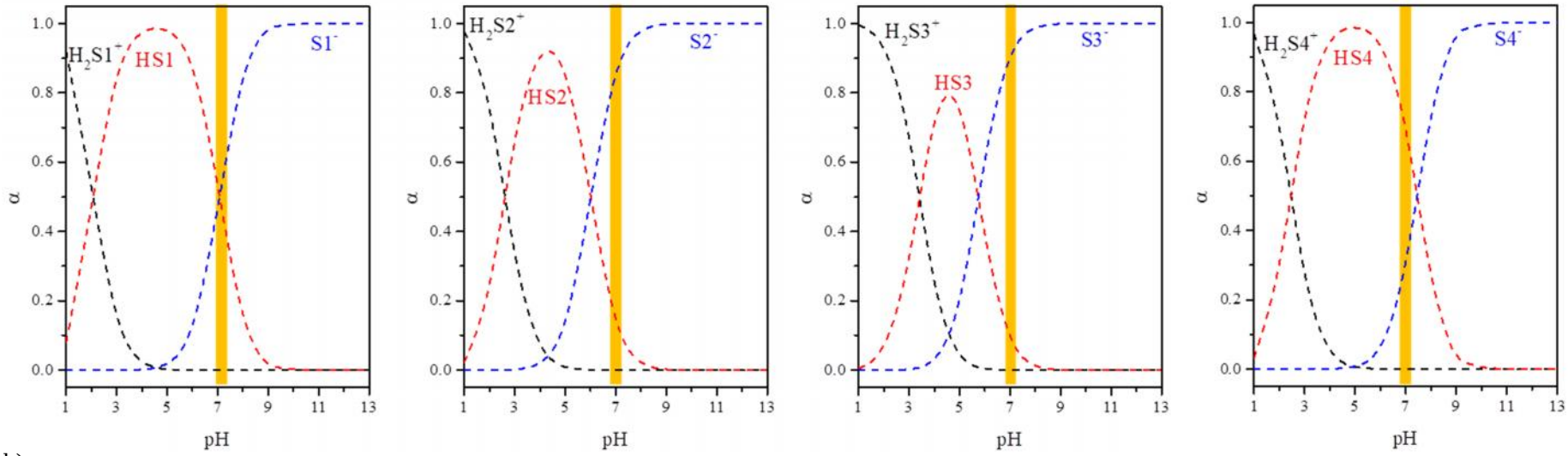


Fig. S3. Van't Hoff plot to calculate the thermodynamic parameters. Conditions: 50 mM Tris-HCl buffer and 100 mM NaCl at pH 7.4.

a)



b)

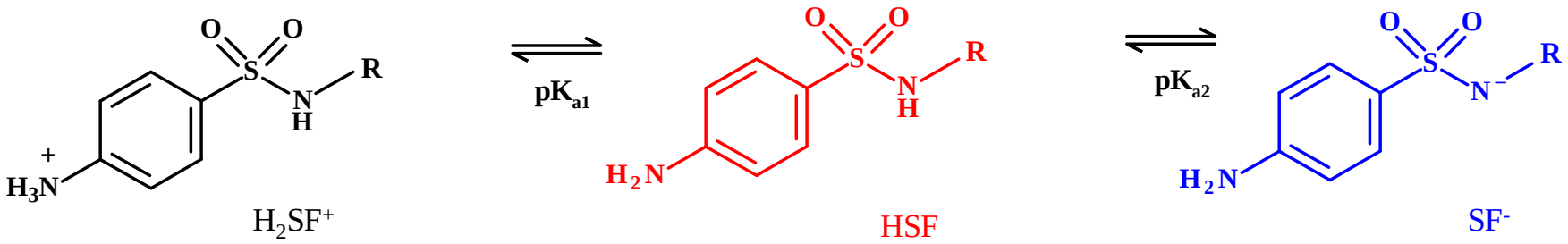


Fig. S4. a) Distribution of sulfonamide species as a function of pH; b) Dissociation equilibrium of sulfonamides (SA).

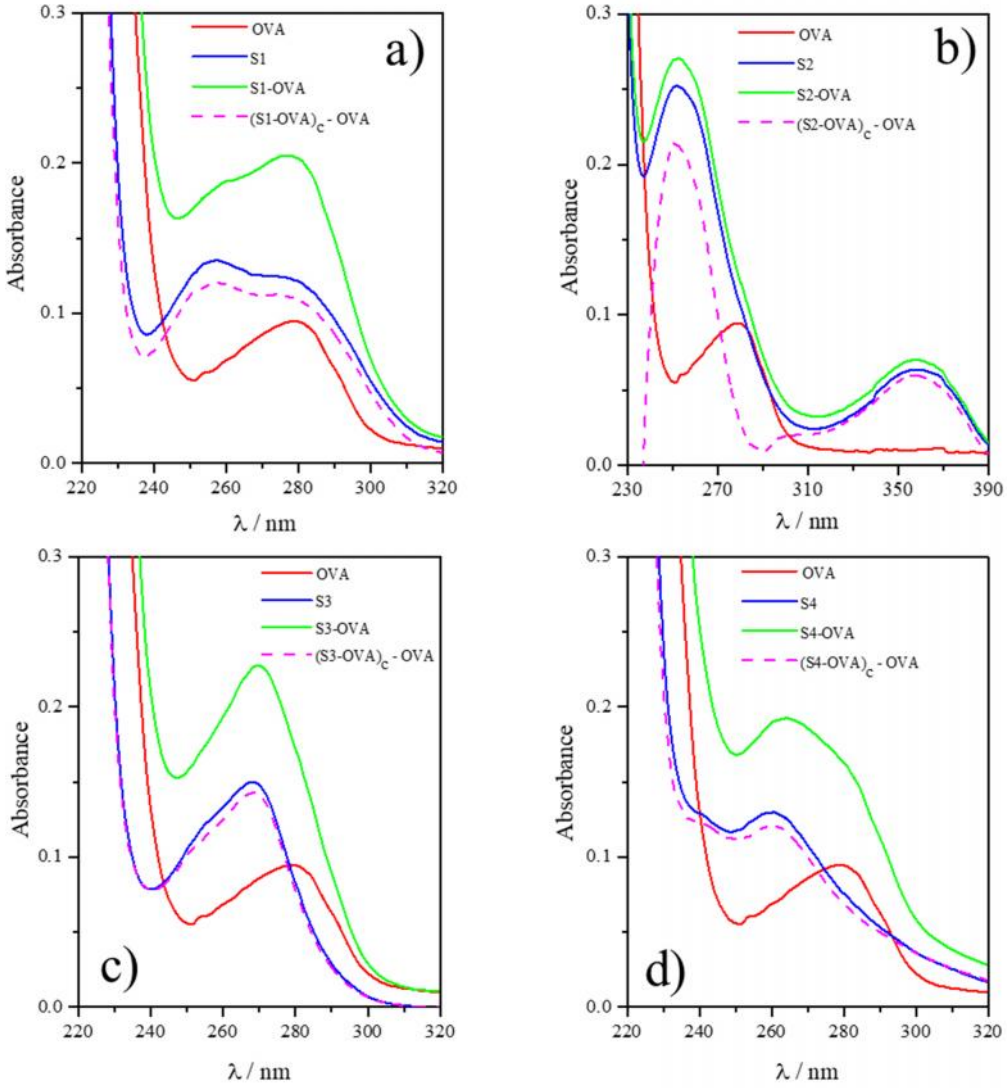


Fig. S5. UV-vis absorption spectra for systems containing a) sulfathiazole (S1), b) sulfaquinoxaline (S2), c) sulfadimethoxine (S3) and d) sulfamethazine (S4). Conditions: OVA (3 μM), sulfonamides (6 μM), 50 mM Tris-HCl buffer and 100 mM NaCl at pH 7.4 and 30ºC.

Table S3
Absorbance values for the sulfonamides evaluated, OVA and OVA-sulfonamide complexes. Conditions: OVA (3 μM), sulfonamides (6 μM), 50 mM Tris-HCl buffer and 100 mM NaCl at pH 7.4 and 30ºC.

Ligand	λ_{max} (nm)	A_{ligand}	A_{OVA}	Comparison		ΔA^*
				$A_{ligand} + A_{OVA}$	$A_{complex}$	
S1	280 (P)	0.1212	0.0944	0.2156	0.2029	- 0.0127
	257 (L)	0.1352	0.0627	0.1979	0.1831	- 0.0148
	278 (PL)	0.1227	0.0943	0.2170	0.2048	- 0.0122
S2	280 (P)	0.1058	0.0944	0.2002	0.1221	- 0.0781
	252 (L)	0.2523	0.0552	0.3075	0.2701	- 0.0374
	253 (PL)	0.2517	0.0598	0.3115	0.2705	- 0.0410
S3	280 (P)	0.0821	0.0944	0.1765	0.1714	- 0.0051
	268 (L)	0.1501	0.0825	0.2326	0.2260	- 0.0066
	269 (PL)	0.1496	0.0844	0.2340	0.2275	- 0.0065
S4	280 (P)	0.0757	0.0944	0.1701	0.1629	- 0.0072
	261 (L)	0.1299	0.0699	0.1998	0.1907	- 0.0091
	264 (PL)	0.1259	0.0752	0.2011	0.1924	- 0.0087

Note: P = protein / L = ligand (sulfonamide) / PL = protein-ligand complex / $^*\Delta A = A_{complex} - (A_{ligand} + A_{OVA})$.

Three-dimensional fluorescence (3D)

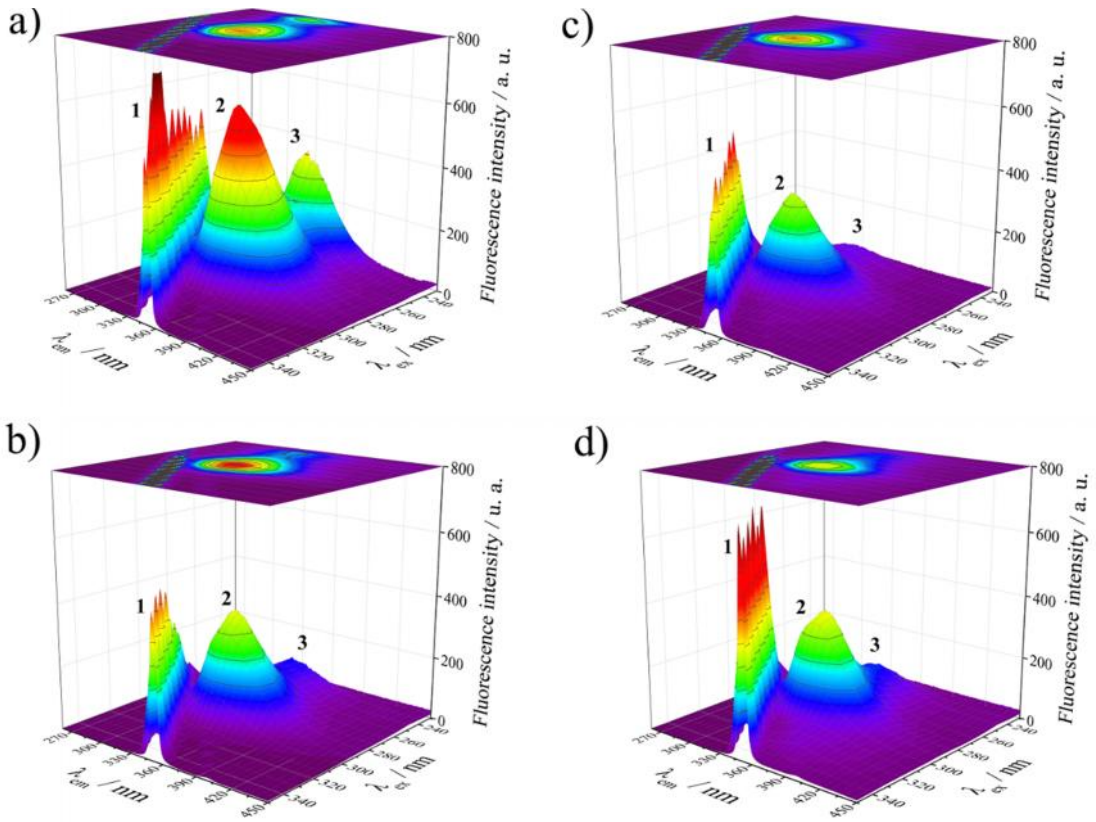


Fig. S6. Three-dimensional fluorescence spectra for a) OVA, b) with addition of S2, c) S3 and d) S4. Conditions: OVA (2 μM), sulfonamides (40 μM), 50 mM Tris-HCl buffer and 100 mM NaCl at pH 7.4 and 30ºC.

Table S4
Parameters associated to the three-dimensional fluorescence spectrum for the interaction between OVA and the sulfonamides evaluated. Conditions: OVA (2 μM), S1 (40 μM), 50 mM Tris-HCl buffer and 100 mM NaCl at pH 7.4 and 30ºC.

System	Peak	Description	Position (λ_{ex} / λ_{em})	Stokes shift $\Delta\lambda$ (nm)	Fluorescence (% reduction)
OVA	1	Rayleigh scattering	$\lambda_{ex} = \lambda_{em}$	0	-
	2	Trp e Tyr	285 / 335	50	575 (100%)
	3	Polypeptide chain	238 / 335	97	360 (100%)
OVA-S1	1	Rayleigh scattering	$\lambda_{ex} = \lambda_{em}$	0	-
	2	Trp e Tyr	285 / 332	47	277 (52%)
	3	Polypeptide chain	238 / 340	102	148 (59%)
OVA-S2	1	Rayleigh scattering	$\lambda_{ex} = \lambda_{em}$	0	-
	2	Trp e Tyr	285 / 332	47	336 (42%)
	3	Polypeptide chain	238 / 335	97	111 (69%)
OVA-S3	1	Rayleigh scattering	$\lambda_{ex} = \lambda_{em}$	0	-
	2	Trp e Tyr	285 / 337	52	372 (35%)
	3	Polypeptide chain	238 / 337	99	131 (64%)
OVA-S4	1	Rayleigh scattering	$\lambda_{ex} = \lambda_{em}$	0	-
	2	Trp e Tyr	285 / 335	50	345 (45%)
	3	Polypeptide chain	238 / 336	98	103 (71%)

Synchronous fluorescence

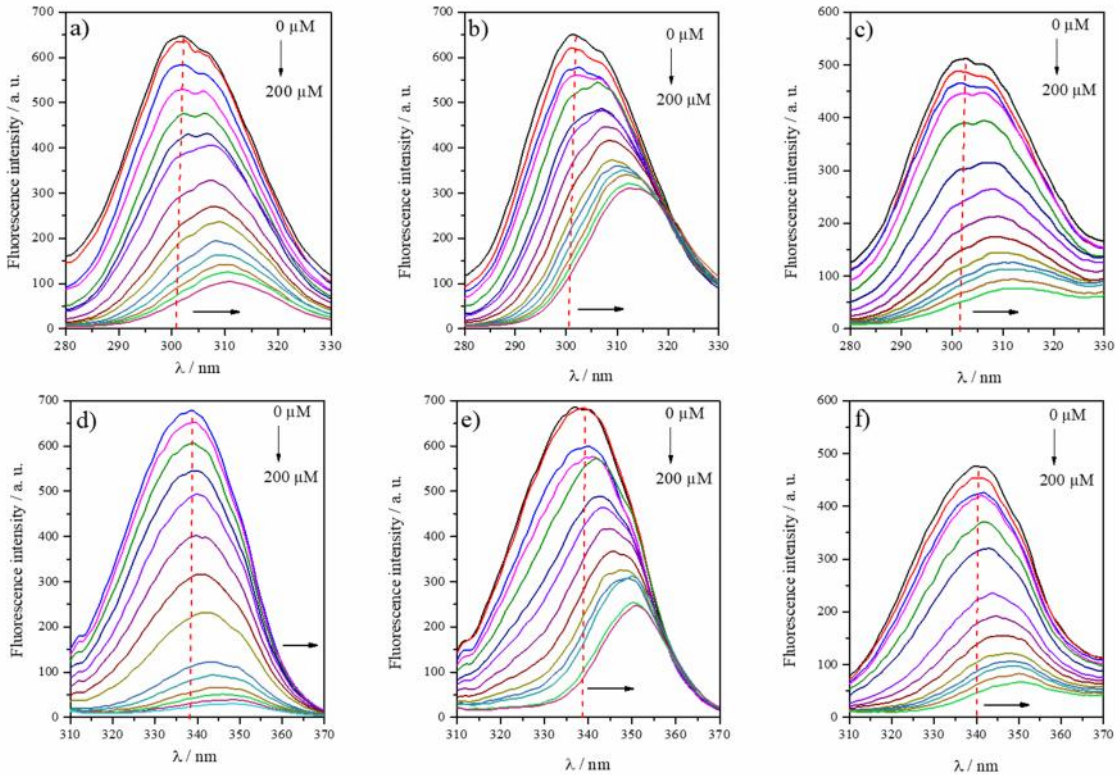


Fig. S7. Synchronous fluorescence for the Tyr residue ($\Delta\lambda$ = 15 nm) with addition a) S2, b) S3 and c) S4 and for the Trp residue ($\Delta\lambda$ = 60 nm) with addition of d) S2, e) S3 and f) S4. Conditions: OVA (2 μM), sulfonamides (0-200 μM), 50 mM Tris-HCl buffer and 100 mM NaCl at pH 7.4 and 30ºC.

Table S5

K_{SV} values for titration by synchronous fluorescence between OVA and the sulfonamides evaluated. Conditions: OVA (2 μM), S1 (0-200 μM), 50 mM Tris-HCl buffer and 100 mM NaCl at pH 7.4 and 30ºC.

Sulfonamides	Δλ (nm)	Maximum variation in λ_{em} (nm)	Ksv (10^4 L mol^{-1})
S1	15	+21	3.52 ± 0.10
	60	+9	3.72 ± 0.21
S2	15	+9	2.24 ± 0.10
	60	+9	3.10 ± 0.24
S3	15	+11	1.55 ± 0.06
	60	+14	1.59 ± 0.07
S4	15	+8	1.78 ± 0.07
	60	+10	1.80 ± 0.01

Förster resonance energy transfer test (FRET)

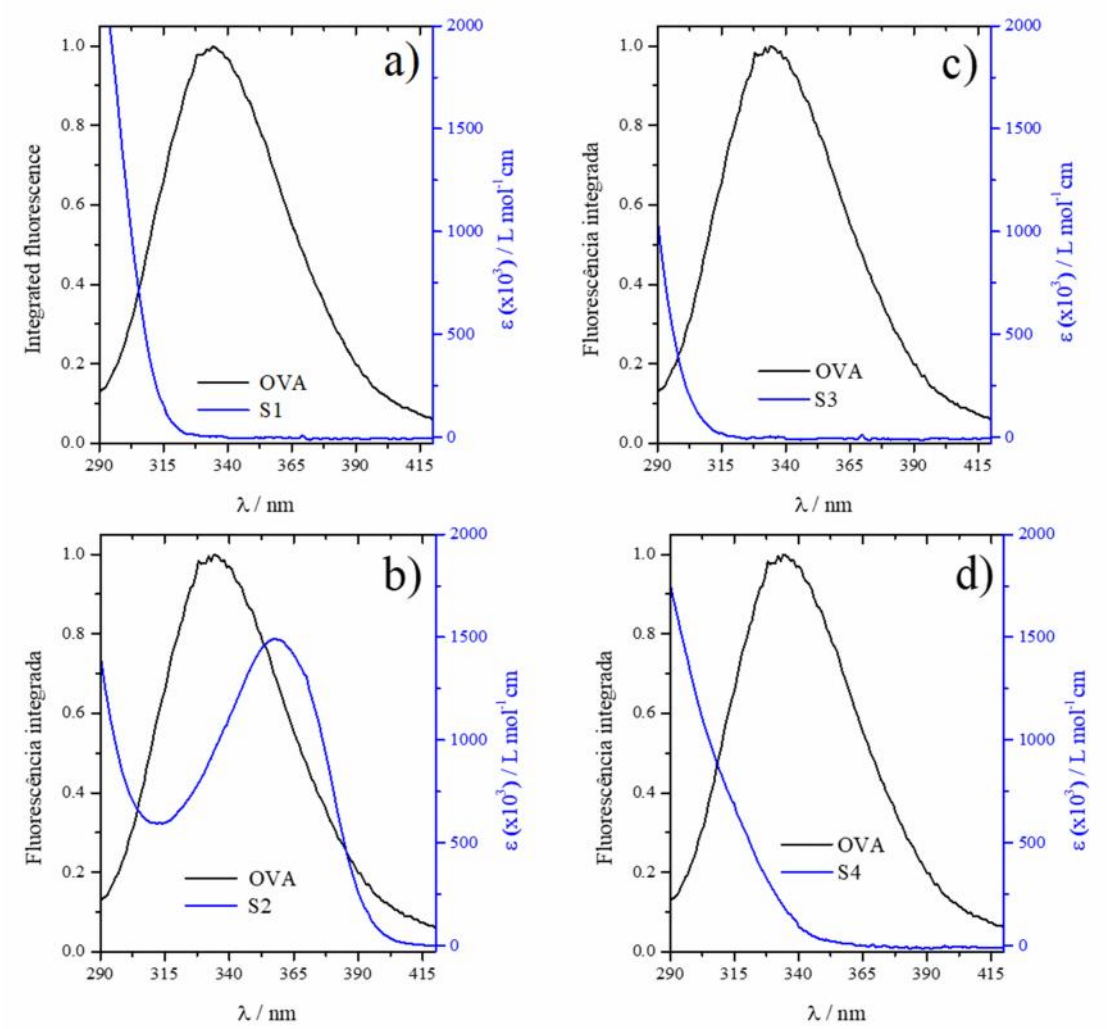


Fig. S8. Spectral overlap of OVA fluorescence emission with the absorption spectrum of a) S1, b) S2, c) S3 and d) S4. Conditions: OVA (2 μM), sulfonamides (10 μM), 50 mM Tris-HCl buffer and 100 mM NaCl at pH 7.4 and 30ºC.

Competition study using the ANS Probe

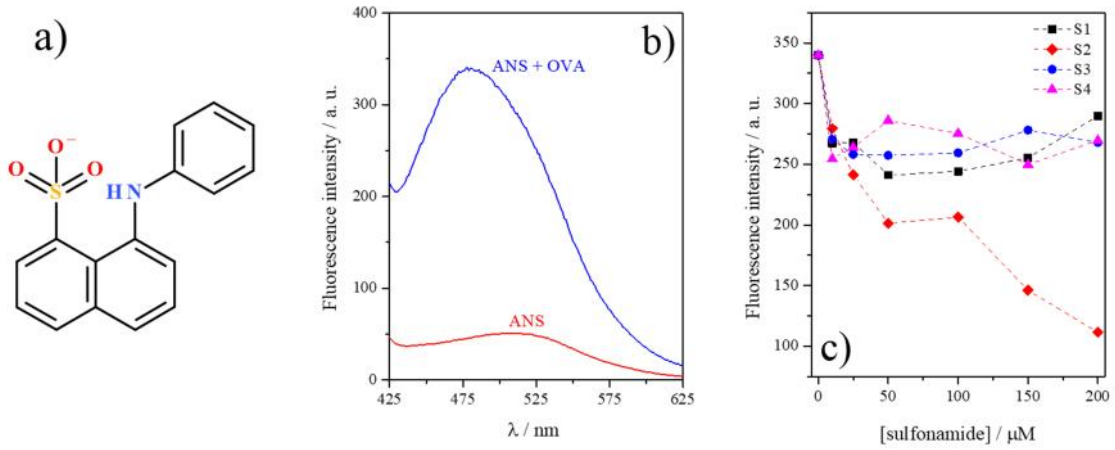


Fig. S9. a) ANS chemical structure, b) ANS fluorescence intensity in the absence and presence of OVA, c) Fluorescence intensity of the ANS-OVA system in the presence of different concentrations of the sulfonamides evaluated. Conditions: OVA (2 μM), ANS (4 μM) sulfonamides (0-200 μM), 50 mM Tris-HCl buffer and 100 mM NaCl at pH 7.4 and 30ºC.

Biological activity

Table S6

Averages of the inhibition halos (in mm) of the growth of the bacteria submitted to the controls and the sulfonamides and their interactions with OVA. Ofloxacin-OFX (5 µg); DMSO; buffer - Tris-HCl (50 mM with 100 mM NaCl at pH 7.4); OVA in buffer (100 µg); S1, S2, S4 (100 µg); S3 (50 µg); interactions OVA-S1, OVA-S2, OVA-S4 (50 µg) and OVA-S3 (25 µg).

Bacterial strains	OFX	DMSO	Buffer	OVA	S1	S1 + OVA	S2	S2 + OVA	S3	S3 + OVA	S4	S4 +O VA
E. coli[*]	33.0 ± 0.0	6.0 ± 2.1	0.0 ± 0.0	-	40.0 ± 0.0	-	32.0 ± 1.4	-	30.0 ± 0.0	-	30.0 ± 0.0	-
E. coli[**]	34.0 ± 1.4	5.0 ± 0.0	0.0 ± 0.0	0.0 ± 0.0	-	39.0 ± 1.4	-	40.0 ± 0.0	-	33.0 ± 4.2	-	34.0 ± 3.5
B. megaterium[*]	33.0 ± 0.0	9.0 ± 0.0	0.0 ± 0.0	-	20.0 ± 0.0	-	18.0 ± 0.0	-	18.0 ± 0.0	-	18.0 ± 0.0	-
B. megaterium[**]	33.0 ± 0.0	12.0 ± 0.0	10.0 ± 0.0	12.0 ± 0.0	-	22.0 ± 0.0	-	21.0 ± 0.0	-	21.0 ± 0.0	-	20.0 ± 0.0
P. aeruginosa[*]	32.0 ± 0.0	12.0 ± 0.0	0.0 ± 0.0	-	12.0 ± 0.0	-	3.0 ± 0.0	-	0.0 ± 0.0	-	0.0 ± 0.0	-
P. aeruginosa[**]	32.0 ± 1.4	11.0 ± 2.1	5.0 ± 0.0	6.0 ± 0.0	-	12.0 ± 0.0	-	12.0 ± 0.0	-	0.0 ± 0.0	-	3.0 ± 0.0
C. glutamicum[***]	33.0 ± 1.1	10.0 ± 0.0	10.0 ± 0.0	10.0 ± 0.0	10.0 ± 0.0	10.0 ± 0.0	10.0 ± 0.0	10.0 ± 0.0	10.0 ± 0.7	14.0 ± 1.4	12.0 ± 0.0	12.0 ± 0.0
K. oxytoca[***]	41.0 ± 1.4	10.0 ± 0.0	10.0 ± 0.0	10.0 ± 0.0	10.0 ± 0.0	10.0 ± 0.0	10.0 ± 0.0	10.0 ± 0.0	10.0 ± 0.0	10.0 ± 0.0	10.0 ± 0.0	10.0 ± 0.0

Notes: [*] Plates with standard, diluents and sulfonamides.
[**] Plates with standard, diluents, OVA and OVA-sulfonamide systems.
[***] Plates with standard, diluents, OVA, sulfonamides and OVA-sulfonamide systems.

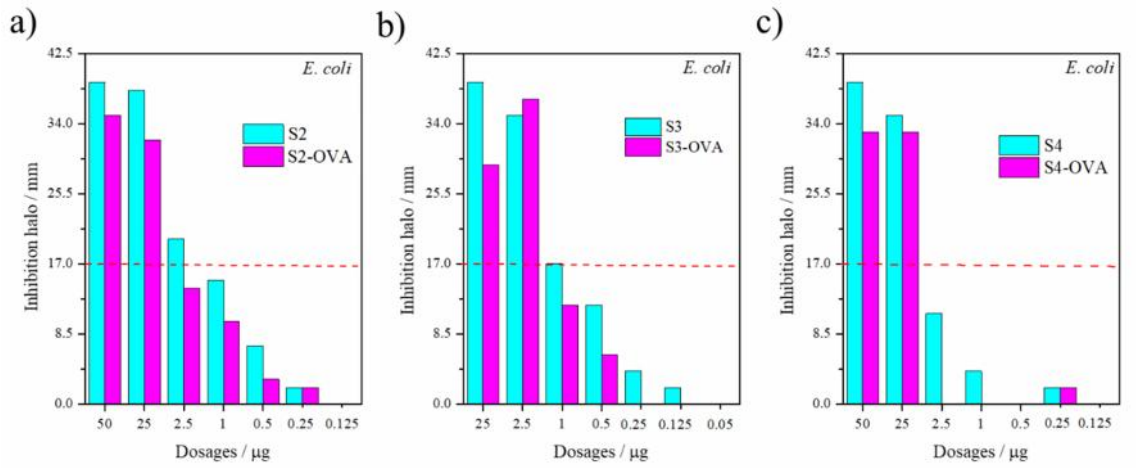


Fig. S10. Inhibition halo values of the different dosages of a) sulfaquinoxaline (S2), b) sulfadimethoxine (S3), c) sulfamethazine (S4) against *Escherichia coli* ATCC 25922.

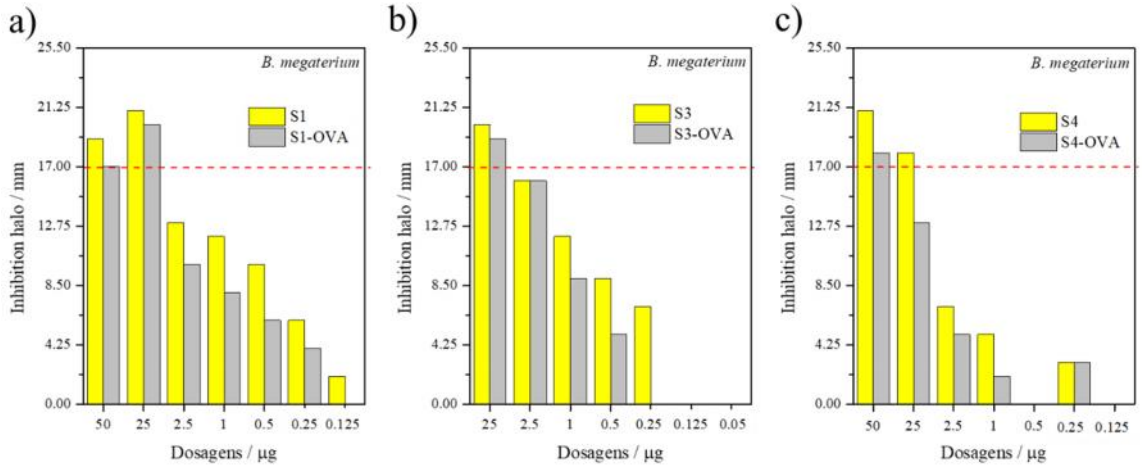


Fig. S11. Inhibition halo values of the different dosages of a) sulfaquinoxaline (S2), b) sulfadimethoxine (S3), c) sulfamethazine (S4) against *Bacillus megaterium* APFSG3isox.

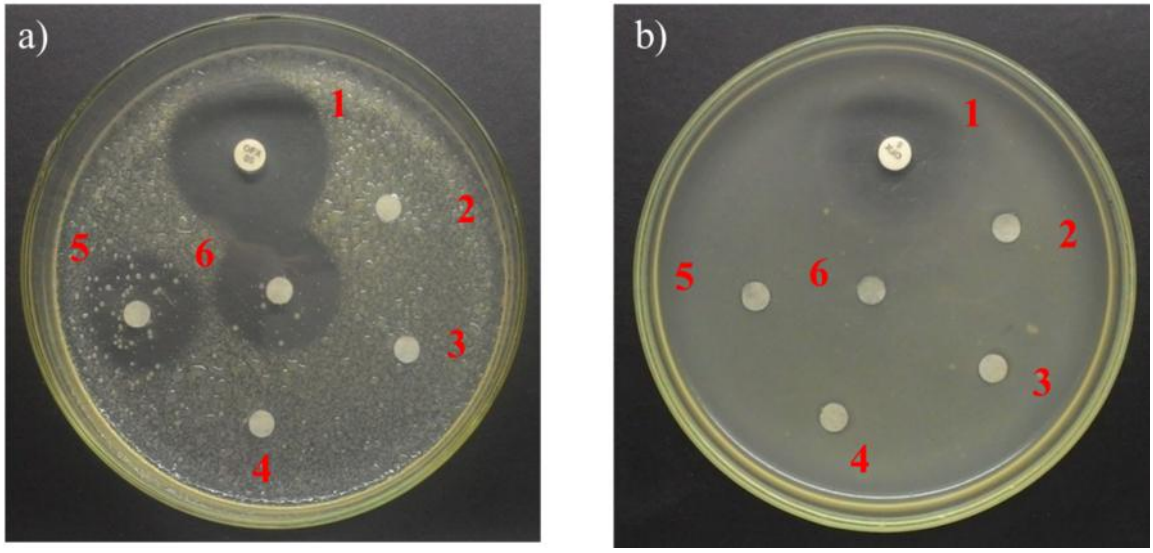


Fig. S12. Aspect of antibiogram against *Escherichia coli* ATCC 25922. Ofloxacin 5 µg (disc 1), DMSO (disc 2), buffer (disc 3), OVA (disc 4), OVA-S1 (disc 5), S1 (disc 6), with S1 dosage equal to a) 2.5 µg, b) 0.125 µg.

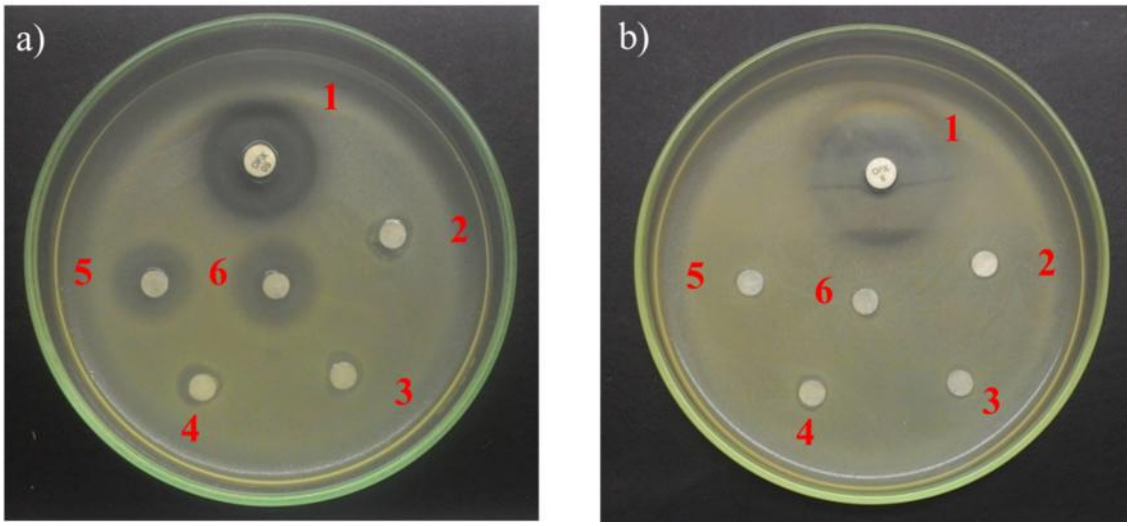


Fig. S13. Aspect of antibiogram against *Bacillus megaterium* APFSG3isox**.** Ofloxacin 5 µg (disc 1), DMSO (disc 2), buffer (disc 3), OVA (disc 4), OVA-S1 (disc 5), S1 (disc 6), with S1 dosage equal to a) 2.5 µg, b) 0.125 µg.

REFERENCES OF THE SUPPLEMENTARY MATERIAL

[1] A.D. Bani-yanseen, Spectrofluorimetric study on the interaction between antimicrobial drug sulfamethazine and bovine serum albumin, J. Lumin. 131 (2011) 1042-1047.

[2] S. Tabassum, W.M. Al-Asbahy, M. Afzal, F. Arjmand, Synthesis, characterization and interaction studies of copper based drug with Human Serum Albumin (HSA): Spectroscopic and molecular docking investigations, J. Photochem. Photobiol., B 114 (2012) 132-139.

[3] J. Chen, X. Zhou, Y. Zhang, H. Gao, Potential toxicity of sulfanilamide antibiotic: Binding of sulfamethazine to human serum albumin, Sci. Total Environ. 432 (2012) 269-274.

[4] M.S. Ali, H.A. Al-Lohedan, Interaction of human serum albumin with sulfadiazine, J. Mol. Liq. 197 (2014) 124-130.

[5] Q. Wang, Sheng-Rui, Zhang, X. Ji, Investigation of interaction of antibacterial drug sulfamethoxazole with human serum albumin by molecular modeling and multi-spectroscopic method, Spectrochim. Acta, Part A 124 (2014) 84-90.

[6] N. Rajendiran, J. Thulasidhasan, Interaction of sulfanilamide and sulfamethoxazole with bovine serum albumin and adenine: Spectroscopic and molecular docking investigations, Spectrochim. Acta, Part A 144 (2015) 183-191.

[7] Y. Lu, Yun-Lai Wang, Sheng-Hua Gao, Gong-Ke Wang, Chang-Ling Yan, De-Jun Chen, Interaction of quercetin with ovalbumin: Spectroscopic and molecular modeling studies, J. Lumin. 129 (2009) 1048-1054.

[8] Rui-qiang Wang, Yu-jing Yin, H. Li, Y. Wang, Juan-Juan Pu, R. Wang, Huan-jing Dou, Chuan-jun Song, Rui-yong Wang, Comparative study of the interactions between ovalbumin and three alkaloids by spectrofluorimetry, Mol. Biol. Rep. 40 (2013) 3409-3418.

[9] F. Shen, F. Niu, J. Li, Y. Su, Y. Liu, Y. Yang, Interactions between tea polyphenol and two kinds of typical egg white proteins – ovalbumin and lysozyme: Effect on the gastrointestinal digestion of both proteins *in vitro*, Food Res. Int. 59 (2014) 100-107.

[10] N. Stanciuc, I. Banu, M. Turturica, I. Aprodu, pH and heat induced structural changes of chicken ovalbumin in relation with antigenic properties, Int. J. Biol. Macromol. 93 (2016) 572-581.

[11] M.D.A. Dantas, H.A. Tenório, T.I.B. Lopes, H.J.V. Pereira, A.J. Marsaioli, I.M. Figueiredo, J.C.C. Santos, Interactions of tetracyclines with ovalbumin, the main allergen protein from egg white: Spectroscopic and electrophoretic studies, Int. J. Biol. Macromol. 102 (2017) 505–514.

[12] P. Manivel, M. Parthiban, M. Ilanchelian, Exploring the binding mechanism between methylene blue and ovalbumin using spectroscopic analyses and computational simulations, J. Biomol. Struct. Dyn. 4 (2019) 1-10.

[13] R. Rajamanikandan A.S. Sharma, M. Ilanchelian, New insights into the binding interaction of food protein ovalbumin with malachite green dye by hybrid spectroscopic and molecular docking analysis, J. Biomol. Struct. Dyn. 19 (2019) 1-12.

[14] Z. Ma, G. Prasanna, L. Jiang, P. Jing, Molecular interaction of cyanidin-3-O-glucoside with ovalbumin: insights from spectroscopic, molecular docking and in vitro digestive studies, J. Biomol. Struct. Dyn. 23 (2019) 1-10.